

# Quantum radiation reaction: Analytical approximations and obtaining the spectrum from moments

Greger Torgrimsson 

Department of Physics, Umeå University, SE-901 87 Umeå, Sweden

 (Received 23 April 2024; accepted 13 September 2024; published 11 October 2024)

We derive analytical  $\chi \ll 1$  approximations for spin-dependent quantum radiation reaction for locally constant and locally monochromatic fields. We show how to factor out fast spin oscillations and obtain the degree of polarization in the plane orthogonal to the magnetic field from the Frobenius norm of the Mueller matrix. We show that spin effects lead to a transseries in  $\chi$ , with powers  $\chi^k$ , logarithms  $(\ln \chi)^k$ , and oscillating terms,  $\cos(\dots/\chi)$  and  $\sin(\dots/\chi)$ . In our approach we can obtain each moment,  $\langle (kP)^m \rangle$ , of the light-front longitudinal momentum independently of the other moments and without considering the spectrum. We show how to obtain a low-energy expansion of the spectrum from the moments by treating  $m$  as a continuous, complex parameter and performing an inverse Mellin transform. We also show how to obtain the spectrum, without making a low-energy approximation, from a handful of moments using the principle of maximum entropy.

DOI: [10.1103/PhysRevD.110.076012](https://doi.org/10.1103/PhysRevD.110.076012)

## I. INTRODUCTION

A common approach to quantum radiation reaction (RR) is to use kinetic equations [1–7], where the rates for constant-crossed fields [8,9] are used as ingredients. See [10] for a review, and [11,12] for other aspects of RR and strong-field QED. In recent years people have realized that spin and polarization effects can be important in various strong-field-QED processes [13–17], and a great deal of work has been done to generalize the previous methods to include spin and polarization, e.g. in particle-in-cell (PIC) codes [17–22]. Stokes vectors have emerged as a useful tool for describing general spin and polarization states. In [23–25] we calculated<sup>1</sup>  $\mathcal{O}(\alpha)$  strong-field-QED Mueller matrices and showed how one can obtain the dominant contribution of higher-orders-in- $\alpha$  processes from products of these matrices. In [26–29] we showed how to resum the resulting  $\alpha$  expansion, resulting in some integro-differential equations for RR. Mueller matrices have now also been incorporated into kinetic equations [30].

This incoherent-product approximation is valid if  $a_0$  is large enough and/or the pulse is sufficiently long. Here<sup>2</sup>

$a_0 = E/\omega$ ,  $E$  is the maximum field strength, and  $1/\omega$  is a characteristic length scale of the field. In this paper we will neglect pair production, which is exponentially suppressed for small  $\chi$ , where  $\chi = \sqrt{-(F^{\mu\nu} p_\nu)^2}$  is the quantum non-linearity parameter.

Recently, the author of [31] presented analytical approximations at next-to-leading order (NLO) in  $\chi \ll 1$  in the locally constant-field (LCF) regime  $a_0 \gg 1$ . In this paper we will calculate analytical approximations at NLO for the resummed Mueller matrix of different moments and for both the LCF regime and for more general regimes, where the incoherent product of  $\mathcal{O}(\alpha)$  Mueller matrices still give the dominant contribution. If  $a_0 \sim 1$ , then this is the case if the pulse is sufficiently long. If the field is almost monochromatic, then one can treat it using a locally monochromatic-field (LMF) approximation [25,32,33] (see also [34]). Such ideas have also been included in some numerical codes [35]. Using LMF is easier for a circularly polarized field. Another reason for considering circular polarization is that spin effects do not average out [27], which they would tend to do for linear polarization. One can also avoid spin effects averaging out by considering various asymmetric oscillations [15,16] or unipolar fields, which can be motivated e.g. by beam-beam collisions [36,37].

We choose coordinates so that the plane wave background field is described by a wave vector  $k_\mu = \omega(1, 0, 0, 1)$  and a polarization vector  $a_\mu(\phi) = \{0, a_1, a_2, 0\}$ , which is in general a pulsed function of light-front time  $\phi = kx = \omega(t + z)$ . In a plane wave the light-front longitudinal momentum  $kP$  plays a key role, where  $P_\mu$  is the momentum of the electron. We can study the dynamics of  $kP$  without considering the transverse components of the momentum  $P_\perp$ . We are in

\*Contact author: [greger.torgrimsson@umu.se](mailto:greger.torgrimsson@umu.se)

<sup>1</sup>We are using the Furry picture, so a  $\mathcal{O}(\alpha)$  term is still a nontrivial/nonperturbative function of the background field  $eF^{\mu\nu}$ .

<sup>2</sup>We use units with  $m_e = c = \hbar = 1$  and absorb  $eF^{\mu\nu} \rightarrow F^{\mu\nu}$ .

Published by the American Physical Society under the terms of the [Creative Commons Attribution 4.0 International license](https://creativecommons.org/licenses/by/4.0/). Further distribution of this work must maintain attribution to the author(s) and the published article's title, journal citation, and DOI. Funded by SCOAP<sup>3</sup>.

particular interested in the moments  $\langle (kP)^m \rangle$ . These expectation values are calculated for a single electron assuming an infinitely sharply peaked wave packet, summed over the probabilities to emit any number of photons. The result can be used as a Green's function for obtaining the corresponding result for a wide wave packet, as explained in [29]. In our approach we obtain  $\langle (kP)^m \rangle$  from a Mueller matrix  $\tilde{\mathbf{M}}(m)$  as

$$\langle (kP)^m \rangle = \frac{1}{2} \mathbf{N}_0 \cdot \tilde{\mathbf{M}} \cdot \mathbf{N}_f, \quad (1)$$

where  $\mathbf{N}_0$  and  $\mathbf{N}_f$  are the initial and final Stokes vectors for the electron spin, which are four-dimensional (4D) vectors  $\mathbf{N} = \{1, \mathbf{n}\}$  where the three-dimensional (3D) vector  $\mathbf{n}$  points in the direction of the spin and where  $0 < \mathbf{n}^2 < 1$  gives the degree of polarization. The Mueller matrix therefore describes the transition from the initial spin to the final spin, much like how ordinary Mueller matrices are used in optics to describe the change in polarization of light beams. Mueller matrices have also been used in QED without a background field [38]. The zeroth moment,  $m = 0$ , gives the probability that an electron which initially has spin described by  $\mathbf{N}_0$  emerges with spin  $\mathbf{N}_f$ ; the first moment,  $m = 1$ , tells us how the average momentum depends on the initial and final spins; and the second moment,  $m = 2$ , is needed to obtain the standard deviation of the momentum distribution. We will consider additional moments in the maximum entropy approach, and complex values of  $m$  in order to obtain the spectrum using an inverse Mellin transform. In [27–29] we derived the following integro-differential equation for the moments:

$$\frac{\partial}{\partial \sigma} \tilde{\mathbf{M}}(b_0) = - \int_0^1 dq \{ \mathbf{M}^L \cdot \tilde{\mathbf{M}}(b_0) + \mathbf{M}^C \cdot \tilde{\mathbf{M}}([1-q]b_0) \}, \quad (2)$$

where  $\sigma$  is a light-front-time variable,  $b_0 = kp$  is the initial longitudinal momentum,  $q = kl/b_0$ , and  $l_\mu$  is the momentum of the emitted or loop photon, and we have “initial” conditions at  $\sigma \rightarrow +\infty$ ,

$$\tilde{\mathbf{M}}(\sigma \rightarrow +\infty, m, b_0) = b_0^m \mathbf{1}_{4 \times 4}. \quad (3)$$

$\mathbf{M}^C$  is the Mueller matrix coming from nonlinear Compton scattering, and  $\mathbf{M}^L$  comes from the electron-mass-operator loop (see Appendix A). The reason  $\mathbf{M}^L$  contributes at the same order as  $\mathbf{M}^C$  is because  $\mathbf{M}^L$  comes from the cross term between the  $\mathcal{O}(\alpha^0)$  and  $\mathcal{O}(\alpha)$  terms in the amplitude [25]. It follows from unitarity that some of the elements of  $\mathbf{M}^L$  are equal to the corresponding elements in  $\mathbf{M}^C$  but with opposite signs. However,  $\mathbf{M}^L$  also contains terms that are not only numerically different from  $\mathbf{M}^C$  but also have a significantly different mathematical structure, as we will show below.

We only need to consider the initial and final spin states at the very end of the calculation, where we obtain the moments by projecting onto the initial and final Stokes vector as in (1). Likewise, we do not need to consider any specific initial wave packet, since the quantities we are considering serve as Green's functions.

We use a tilde on  $\tilde{\mathbf{M}}(b_0, m)$  to distinguish the moments from the cumulative distribution  $\mathbf{M}(b_0, x)$ , which gives the probability that the final momentum  $kP$  is larger than some fraction of the initial momentum  $kp$ ,

$$kP > (1-x)kp. \quad (4)$$

The spectrum is obtained from  $\mathbf{S} = \partial_x \mathbf{M}(b_0, x)$ , so  $x$  is directly related to the final momentum  $kP$ , but is scaled so that  $0 < x < 1$ . As explained in [29], it is often easier to first calculate  $\mathbf{M}$  and then take the  $x$  derivative at the end, rather than working directly with  $\mathbf{S}$ .

Note that, in contrast to the usual kinetic equations, with (2) we treat each moment separately. There is no hierarchy relating one moment to other moments, and we do not need to compute the spectrum. So, if we want to calculate e.g. the second moment, then we only have to consider the second moment. Another thing to note is that (2) is integrated backwards in (light-front) time. Thus, while we showed in [29] that (2) is consistent with the standard kinetic approach, (2) provides a genuinely different approach. Given that we can obtain the moments independently, a relevant question is to what extent we can reproduce the spectrum from knowledge of the moments. In this paper we study two different ways of doing so, by (1) treating  $m$  as a complex Mellin variable or (2) using the principle of maximum entropy.

This paper is organized as follows. In Sec. II we calculate the first couple of terms in the  $\chi \ll 1$  expansion of the moments  $\tilde{\mathbf{M}}(m)$  in the LCF regime, and we explain two methods for calculating the exact  $\tilde{\mathbf{M}}$  numerically. In Sec. III we show how to obtain the  $\chi \ll 1$  expansion of the spectrum by treating  $m$  as a complex, Mellin integration variable. In Sec. IV we show how to use the principle of maximum entropy to obtain the spectrum from  $\tilde{\mathbf{M}}(m)$  with only a handful of moments  $m$ . In Sec. V we calculate the leading quantum correction beyond the LCF regime, i.e. for a sufficiently long field but without assuming  $a_0 \gg 1$ . In Sec. VI we show how to factor out fast spin oscillations for a linearly polarized field in the LCF regime and obtain the degree of polarization from the Frobenius norm of the Mueller matrix.

## II. LCF APPROXIMATION OF MOMENTS

We first consider the LCF regime,  $a_0 \gg 1$ . We use the same idea as in Eq. (77) in [29]; i.e. we first factor out the overall  $b_0^m$  scaling as

$$\tilde{\mathbf{M}}(\sigma, m, b_0) =: b_0^m \mathbf{W}(\sigma, m, b_0). \quad (5)$$

From (3) we have

$$\mathbf{W}(\sigma \rightarrow +\infty, m, b_0) = \mathbf{1}, \quad (6)$$

i.e. the same ‘‘initial’’ conditions for all moments. Different moments  $\mathbf{W}(m)$  and  $\mathbf{W}(m')$  are now typically on the same order of magnitude (unless some of the components vanish identically to some order, which we will see examples of below). The equation of motion now depends explicitly on  $m$ ,

$$\begin{aligned} \frac{\partial}{\partial \sigma} \mathbf{W}(b_0) = & - \int_0^1 dq \{ \mathbf{M}^L \cdot \mathbf{W}(b_0) \\ & + (1-q)^m \mathbf{M}^C \cdot \mathbf{W}([1-q]b_0) \}. \end{aligned} \quad (7)$$

At this point we have not yet assumed the LCF regime. In LCF, the Mueller matrices  $\mathbf{M}^{L,C}$  are given in Appendix A and are expressed in terms of a locally constant value of the quantum nonlinearity parameter,

$$\chi(\sigma) = |\mathbf{a}'(\sigma)| b_0 = \chi_0 F(\sigma), \quad (8)$$

where  $\chi_0 = a_0 b_0$  is the maximum value of  $\chi$  and  $F$  is a dimensionless function, e.g.  $F(x) = e^{-x^2}$ . We consider for simplicity a linearly polarized field, so that the magnetic field is always either parallel or antiparallel to a constant, unit vector  $\hat{\mathbf{B}}_0$ ,

$$\hat{\mathbf{B}}(\sigma) = \epsilon(\sigma) \hat{\mathbf{B}}_0, \quad (9)$$

where  $\epsilon(\sigma) = \pm 1$  depending on the sign of  $a'(\sigma)/|a'(\sigma)|$ . The 4D Stokes vectors live in a vector space that is spanned by  $\hat{\mathbf{B}}_0 = -\mathbf{e}_2$ , the electric field direction  $\hat{\mathbf{E}}_0 = \mathbf{e}_1$ , the propagation direction  $\hat{\mathbf{k}} = \mathbf{e}_3$ , and a vector that describes an unpolarized electron  $\mathbf{e}_0$ . For a linearly polarized field, the  $\mathbf{e}_0 - \hat{\mathbf{B}}_0$  components decouple from the  $\hat{\mathbf{E}}_0 - \hat{\mathbf{k}}$  components. In this section we will only consider the  $\mathbf{e}_0 - \hat{\mathbf{B}}_0$  components. We consider the  $\hat{\mathbf{E}}_0 - \hat{\mathbf{k}}$  components in Sec. VI. Since we will only consider the  $\mathbf{e}_0 - \hat{\mathbf{B}}_0$  subspace in this section, we will only present the components of the Mueller matrices which act on this subspace. In other words, rather than presenting the full 4D Mueller matrices, we present the block part which acts on the two-dimensional (2D) subspace. To avoid cluttering the notation, we will denote the 2D matrices with  $\mathbf{M}$  rather than e.g.  $\mathbf{M}_{2D}$ . We order the components such that  $\mathbf{e}_0 = \{1, 0\}$  and  $\hat{\mathbf{B}}_0 = \{0, 1\}$ . So, for example,  $M_{11} = \mathbf{e}_0 \cdot \mathbf{M} \cdot \mathbf{e}_0$  corresponds to a probability summed/averaged over both the initial and the final spins;  $M_{12} = \mathbf{e}_0 \cdot \mathbf{M} \cdot \hat{\mathbf{B}}_0$  ( $M_{21} = \hat{\mathbf{B}}_0 \cdot \mathbf{M} \cdot \mathbf{e}_0$ ) gives the difference in the probability when comparing the two cases where the final (initial) spin is either up or down, while the initial (final) spin is unpolarized; and if the initial beam is completely polarized with spin up

and the detector only measures final states with spin up, then one would be interested in  $\{1, 1\} \cdot \mathbf{M} \cdot \{1, 1\} = M_{11} + M_{12} + M_{21} + M_{22}$ .

In the constant-field case [29], we defined a ‘‘time’’ or pulse-length parameter  $u$ , such that the longitudinal component of the solution to the LL equation is given by  $kP_{LL}/b_0 = 1/(1+u)$ , i.e.  $u = (2/3)\chi\alpha a_0 \Delta\sigma$ . Note that  $u$  is proportional to  $\chi$  or  $b_0$ , but we want to consider  $u = \mathcal{O}(1)$  even when  $\chi \ll 1$ , because otherwise we would not see the nontrivial dependence on  $u$  and the results, which are in general all orders in  $\alpha$ , would just reduce to  $\mathcal{O}(\alpha)$ . Now when we consider nonconstant fields, we cannot use the same  $u$  variable, but we still want to capture the nontrivial dependencies. To do so we define

$$\rho := \frac{2}{3} \alpha b_0 a_0^2, \quad (10)$$

which we consider to be  $\mathcal{O}(1)$ , which is the case if  $a_0$  is sufficiently large to compensate for  $\alpha \ll 1$  and  $b_0 \ll 1$ . Our results below are still valid if  $\rho$  is smaller, but then they simply reduce to  $\mathcal{O}(\alpha)$ . Then we expand the solution as a power series in  $\chi_0$ ,

$$\mathbf{W}(\sigma, \chi_0, m) = \sum_{k=0}^{\infty} \mathbf{w}_{m,k}(\sigma, \rho) \chi_0^k, \quad (11)$$

but where the coefficients are still nontrivial functions of  $\rho$ . We will show in Sec. VI that the  $\hat{\mathbf{E}}_0 - \hat{\mathbf{k}}$  components of  $\mathbf{W}$  also contain terms with  $\ln \chi_0$  and  $\cos(\dots/\chi_0)$  or  $\sin(\dots/\chi_0)$ , so the results have in general a nontrivial transseries structure. From  $\mathbf{M}^{L,C}$  we have an overall factor of  $\alpha/b_0 = (3/2)(\rho/\chi_0^2)$  on the right-hand side of (7). When  $b_0$  decreases, the relevant integration interval for  $q$  shrinks, so  $q$  is not a natural variable for calculating the  $b_0 \ll 1$  expansion. We therefore change variable from  $q$  to  $\gamma$ , where

$$q = \frac{b_0 \gamma}{1 + b_0 \gamma}, \quad (12)$$

so that we can expand the integrand in (7) in a series in  $b_0$  with  $\gamma$  as independent of  $b_0$ . To zeroth order we find

$$\mathbf{w}_{m,0} = \frac{\mathbf{1}}{(1 + \rho J(\sigma))^m}, \quad (13)$$

where

$$J(\sigma) = \int_{\sigma}^{\infty} d\sigma' F^2(\sigma'). \quad (14)$$

Note that it is the lower rather than upper integration limit that is given by  $\sigma$ , because our equations for the moments are integrated backwards in time. Equation (13) is, though,

exactly what one would expect<sup>3</sup> from the exact solution to the classical Landau-Lifshitz (LL) equation [39,40].

After expanding (7) to the next-to-leading order, we find a partial differential equation which involves both  $\partial_\sigma \mathbf{w}$  and  $\partial_\rho \mathbf{w}$ . We can make this an ordinary differential equation using the method of characteristics; i.e. we change variables from  $\sigma$  and  $\rho$  to  $t = \sigma$  and

$$y = \frac{1}{\rho} + J(\sigma). \quad (15)$$

After this change of variables we have an equation in the form

$$(y - J)^{m+2} \frac{\partial}{\partial t} \frac{\mathbf{w}_{m,1}}{(y - J)^{m+1}} = F^3 \mathbf{R}(J, y), \quad (16)$$

where  $\mathbf{R}$  is a rational function of  $J$  and  $y$  [the explicit expression for  $\mathbf{R}$ , obtained by expanding (7), is not illuminating]. It is now straightforward to integrate (16). We find for the zeroth, first, and second moments

$$\mathbf{w}_{0,1} = \int_{-\infty}^{\infty} d\sigma \frac{\rho F^3(\sigma)}{[1 + \rho I(\sigma)]^2} \frac{3}{2} \begin{pmatrix} 0 & \epsilon(\sigma) \\ 0 & -\frac{5\sqrt{3}}{8} \end{pmatrix}, \quad (17)$$

$$\mathbf{w}_{1,1} = \int_{-\infty}^{\infty} d\sigma \frac{\rho F^3(\sigma)}{[1 + \rho I(\infty)]^2} \begin{pmatrix} \frac{55}{16\sqrt{3}} \left( \frac{1}{1 + \rho I(\infty)} + \frac{2}{1 + \rho I(\sigma)} \right) & \frac{3\rho I(\infty) - I(\sigma)}{2[1 + \rho I(\sigma)]^2} \epsilon(\sigma) \\ -\frac{3}{2[1 + \rho I(\sigma)]} \epsilon(\sigma) & \frac{55}{16\sqrt{3}} \left( \frac{1}{1 + \rho I(\infty)} + \frac{2}{1 + \rho I(\sigma)} \right) - \frac{15\sqrt{3}[1 + \rho I(\infty)]}{16[1 + \rho I(\sigma)]^2} \end{pmatrix}, \quad (18)$$

$$\mathbf{w}_{2,1} = \int_{-\infty}^{\infty} d\sigma \frac{\rho F^3(\sigma)}{[1 + \rho I(\infty)]^3} \begin{pmatrix} \frac{55}{16\sqrt{3}} \left( \frac{3}{1 + \rho I(\infty)} + \frac{4}{1 + \rho I(\sigma)} \right) & -\frac{3(1 + 2\rho I(\sigma) - \rho I(\infty))}{2[1 + \rho I(\sigma)]^2} \epsilon(\sigma) \\ -\frac{3}{1 + \rho I(\sigma)} \epsilon(\sigma) & \frac{55}{16\sqrt{3}} \left( \frac{3}{1 + \rho I(\infty)} + \frac{4}{1 + \rho I(\sigma)} \right) - \frac{15\sqrt{3}[1 + \rho I(\infty)]}{16[1 + \rho I(\sigma)]^2} \end{pmatrix}, \quad (19)$$

where we have used

$$J(-\infty) - J(\sigma) = \int_{-\infty}^{\sigma} d\sigma' F^2(\sigma') := I(\sigma). \quad (20)$$

For a constant field these results reduce to Eqs. (92), (74), and (75) in [29].

If the field oscillates in a symmetric fashion, then the off-diagonal elements of the above matrices tend to vanish upon integration over  $\sigma$ , due to the  $\epsilon(\sigma)$  factors. This means, in particular, that there would be no Sokolov-Ternov effect<sup>4</sup>; i.e. if the initial electron is unpolarized ( $\mathbf{N} = \{1, 0\}$ ), then it will stay unpolarized. It also means that if we sum over the final spin states, then there is no dependence on the initial spin. However, this does not mean that all spin effects are gone. If, for example, the initial state is completely polarized along the magnetic field axis,  $\mathbf{N} = \{1, s\}$ , where  $s = \pm 1$ , then after interaction there is a nonzero probability to find the electron in the spin-flipped state  $\mathbf{N} = \{1, -s\}$ . So, if one prepares the initial electron to

be spin up and the detector only measures electrons with spin up, then the resulting RR is different from the unpolarized case. This also means that an initially polarized beam tends to become depolarized.

If we sum over the final spin, then, as in the constant-field case, we find that the standard deviation does not depend on the initial spin. We find

$$S^2 = \frac{55\rho\chi_0}{16\sqrt{3}[1 + \rho I(\infty)]^4} \int_{-\infty}^{\infty} d\sigma F^3(\sigma). \quad (21)$$

Equation (21) agrees with Eq. (14) in [31]. We make further comparison in Appendix C.

We compare the analytical results in (17) and (18) with the exact, numerical results in Figs. 1 and 2 for  $\chi_0 = 10^{-3}$ . We have chosen such a small  $\chi_0$  to make sure that the agreement is precise. We have obtained the numerical results in two very different ways.

### A. Direct numerical computation

One way is to solve (2) by performing the integration over  $\sigma$  using e.g. the midpoint method. At each point in  $\sigma$  we make an interpolation function for the dependence on  $\chi_0$  in the interval  $0 < \chi_0 < \chi_{\max}$ . Since we are often interested in small  $\chi_{\max}$  and several different moments, rescaling and subtracting as follows helps with the precision and accuracy of the numerical computation. First of all, we use (7) instead of (2), since  $\mathbf{W}$  is on the same order of magnitude

<sup>3</sup>Agreement between LL and the classical limit of kinetic equations in the LCF regime has been demonstrated in [3,4,7]. In [26] it was also shown that the classical limit of the incoherent-product approximation, which we are using here, agrees with LL beyond the LCF regime.

<sup>4</sup>The standard Sokolov-Ternov result [41,42] for the induced polarization is actually for a case without RR, while here we consider induced polarization with RR.

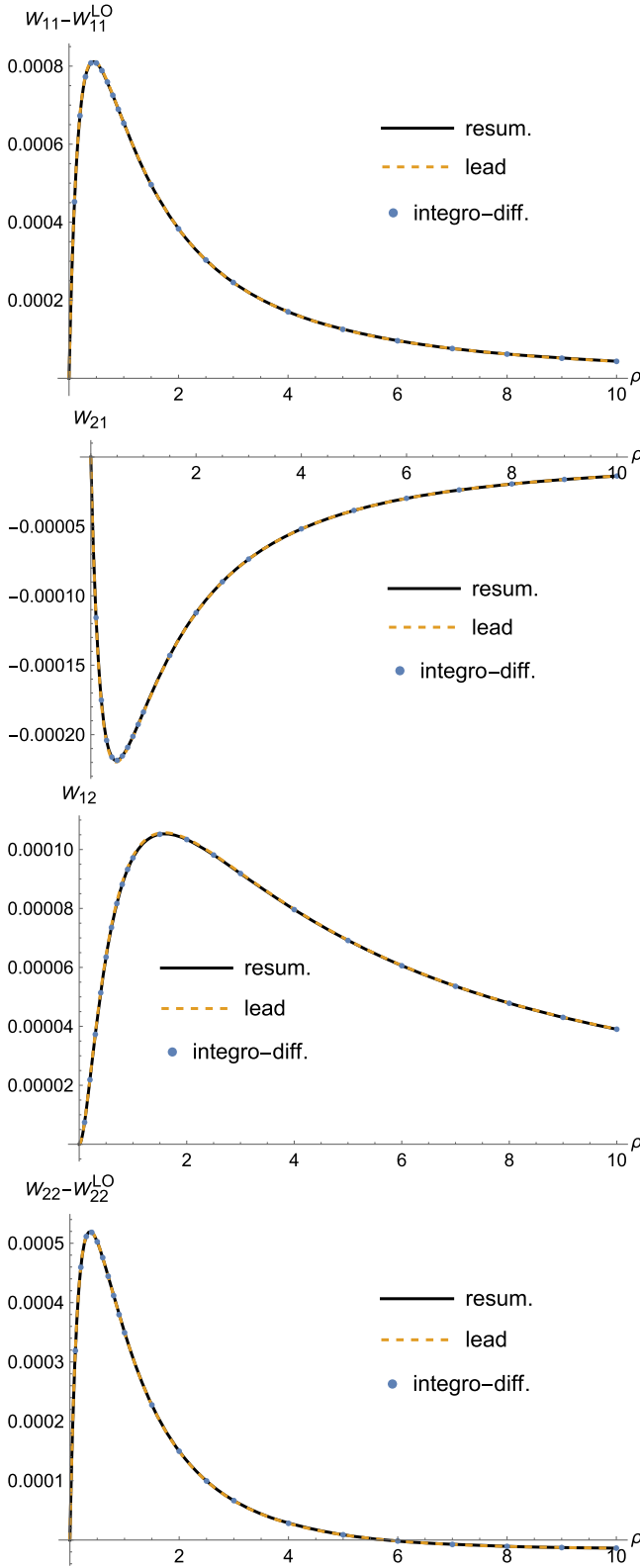


FIG. 1. The first moment,  $\mathbf{W}(m=1)$  for a Sauter pulse and  $\chi_0 = 10^{-3}$ , for the components  $W_{11} = \mathbf{e}_0 \cdot \mathbf{W} \cdot \mathbf{e}_0$ ,  $W_{12} = \mathbf{e}_0 \cdot \mathbf{W} \cdot \hat{\mathbf{B}}_0$ , etc. The “lead” curves show the analytical result for the leading order in (18). The “integro-diff.” curves are numerical solutions to (2). The “resum.” curves are obtained with the double resummation approach.

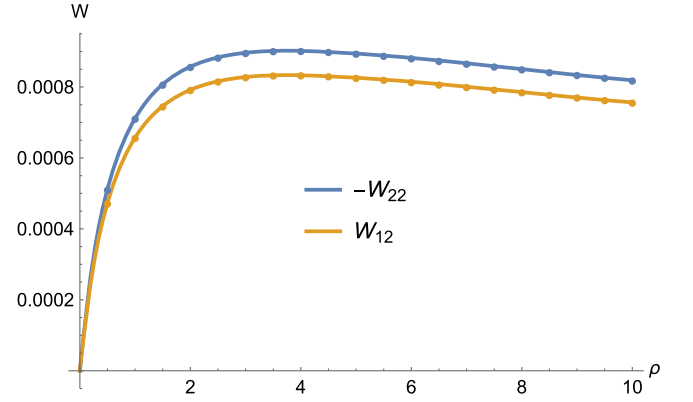


FIG. 2. The zeroth moment,  $\mathbf{W}(m=0)$ , for a Sauter pulse and  $\chi_0 = 10^{-3}$ . The solid lines are the leading order from (17), and the dots are numerical solutions to (2).

for all moments, while  $\mathbf{M}$  decreases by orders of magnitude due to the overall  $b_0^m$  scaling, so in terms of  $\mathbf{W}$  we can work with the same accuracy for different  $m$ . We change integration variable from  $q = \chi Y^3 / (1 + \chi Y^3)$  to  $Y$ . This makes the interval which gives a significant contribution to the integral  $\mathcal{O}(\chi^0)$ . In contrast, in terms of  $q$  the numerically important region would become smaller and smaller when we decrease  $\chi$ . Moreover, since we already know that the zeroth order is given by (13), we subtract it in order to not waste precision and time computing it numerically. We therefore write

$$\mathbf{W} =: \mathbf{w}_{m,0} + \chi_0 \Delta \mathbf{W} \quad (22)$$

and rewrite (7) as (omitting the  $m$  subscript on  $\mathbf{w}_{m,0}$ )

$$\begin{aligned} \partial_\sigma \Delta \mathbf{W} = & - \int_0^\infty dY \mathcal{J} \left\{ \mathbf{M}_L \cdot \Delta \mathbf{W}(b_0) \right. \\ & + (1-q)^{m+1} \mathbf{M}_C \cdot \Delta \mathbf{W}([1-q]b_0) \\ & + \frac{1}{\chi_0} \left( \mathbf{M}_L \cdot \mathbf{w}_0(b_0) + (1-q)^m \mathbf{M}_C \cdot \mathbf{w}_0([1-q]b_0) \right. \\ & \left. \left. + \frac{1}{\mathcal{J}} [\mathcal{J} q \mathbf{M}_C]_{\text{lead}} \cdot \left[ m \mathbf{w}_0 + b_0 \frac{\partial \mathbf{w}_0}{\partial b_0} \right] \right) \right\}, \quad (23) \end{aligned}$$

where  $\mathcal{J} = 3\chi Y^2(1 + \chi Y^3)^2$  is the Jacobian for the change of integration variable and

$$[\mathcal{J} q \mathbf{M}_C]_{\text{lead}} = - \frac{9\chi^2 \rho}{2\chi_0^2} [Y^5 \text{Ai}_1(Y^2) + 2Y^3 \text{Ai}'(Y^2)] \mathbf{1} \quad (24)$$

is obtained by expanding  $\mathcal{J} q \mathbf{M}_C$  to leading order in  $\chi_0 \ll 1$  with  $Y = \mathcal{O}(\chi_0^0)$ . The term in the last row of (23) is exactly equal to  $-\partial_\sigma \mathbf{w}_0$ . The reason for writing it as this  $Y$  integral of (24) is that it cancels the leading order of the third row, so the  $\mathcal{O}(1/\chi_0)$  terms cancel already on the integrand level. Equation (23) might look more complicated than (7), but

(23) is more convenient for numerical computation because the precision and accuracy goals of the integral are the same as that of  $\Delta\mathbf{W}$ . In contrast, if we instead solve (7) in terms of  $\mathbf{W}$ , then for  $\chi \ll 1$  we lose precision when we subtract the leading order,  $\mathbf{W} - \mathbf{w}_0$ .

For the particular example of a Sauter pulse,  $a_\mu = \{0, a, 0, 0\}$  with

$$a(\sigma) = a_0 \tanh(\sigma), \quad F(\sigma) = \text{sech}^2(\sigma), \quad (25)$$

we changed variable from  $\sigma$  to  $t = \tanh(\sigma)$  and then integrated from  $t = 1$  to  $t = -1$  with step size  $\Delta t = 1/100$ . We solved (23) for a couple of different values of  $T = \alpha a_0 = (3/2)(\rho_0/\chi_{\max})$  with  $\rho_0 = \{0.1, 0.2, \dots, 1, 1.5, 2, 2.5, 3, 4, \dots, 10\}$  shown by dots in Fig. 1.

## B. Double resummation approach

The second method is to make a double resummation, where we express  $\tilde{\mathbf{M}}$  in terms of its Taylor series in  $\alpha$ ,

$$\tilde{\mathbf{M}} = \sum_{n=0}^{\infty} \tilde{\mathbf{M}}^{(n)}, \quad (26)$$

where  $\tilde{\mathbf{M}}^{(n)}$  is proportional to  $\alpha^n$ .  $\tilde{\mathbf{M}}^{(n)}$  is obtained from  $\tilde{\mathbf{M}}^{(n-1)}$  using the recursive equation

$$\begin{aligned} \tilde{\mathbf{M}}^{(n)}(b_0, \sigma) = & \int_{\sigma}^{\infty} d\sigma' \int_0^1 dq \{ \mathbf{M}^L(\sigma') \cdot \tilde{\mathbf{M}}^{(n-1)}(b_0, \sigma') \\ & + \mathbf{M}^C(\sigma') \cdot \tilde{\mathbf{M}}^{(n-1)}([1-q]b_0, \sigma') \}, \end{aligned} \quad (27)$$

starting with

$$\tilde{\mathbf{M}}^{(0)}(m, b_0) = b_0^m \mathbf{1}. \quad (28)$$

The idea is to solve (27) to obtain the first, say, 10 or 15 orders, and then resum the  $\alpha$  expansion using Padé approximants. While (27) can be solved by making a numerical interpolation function for the dependence on  $\chi_0$  of each  $\tilde{\mathbf{M}}^{(n)}$ , we have instead solved it by making a second expansion,

$$\tilde{\mathbf{M}}^{(n)}(m) = \sum_k \chi_0^k \tilde{\mathbf{M}}^{(n,k)}. \quad (29)$$

For a Sauter pulse we can analytically obtain each coefficient  $\tilde{\mathbf{M}}^{(n,k)}$  in this double expansion. We again change variable from  $\sigma$  to  $t = \tanh(\sigma)$ , and then, after expanding in  $\chi_0$ , we find integrals of the form

$$\int_t^1 dt' t'^j = \frac{1}{1+j} (1 - t^{1+j}), \quad (30)$$

with integer  $j$ . This simple formula is the main reason why we chose a Sauter field. We have obtained the first 40

orders in  $\chi_0$  for each  $\tilde{\mathbf{M}}^{(n)}$  up to  $n = 15$ . We then resum the  $\chi_0$  expansions for each  $\tilde{\mathbf{M}}^{(n)}$  separately using the Borel-Padé method, and finally we resum the  $\alpha$  expansion using Padé approximants. We need the full “time”  $t$  dependence of  $\mathbf{M}^{(n)}$  in order to calculate  $\mathbf{M}^{(n+1)}$ , so, in the intermediate steps in the calculation,  $\tilde{\mathbf{M}}^{(n,k)}$  are functions of  $t$ , while they would be just constants for a constant field. However, after we have obtained all 10 or 15 orders we evaluate all these functions at  $t = -1$ . Thus, the actual resummations, using Borel-Padé and Padé, are essentially the same as in the constant field case. We therefore refer to [26,27] for more details. The results are shown in black lines in Fig. 1. The precise agreement with the leading analytical  $\mathcal{O}(\chi)$  results shows that in this particular regime it is unnecessary to resum the  $\chi$  expansions.

As a more nontrivial check of the resummation approach, we consider  $\chi_0 = 1/2$ . To check the resummation of the  $\chi$  expansions we have used two completely different methods: the standard Padé-Borel method (see e.g. [43]) and the method proposed in [44]. For the example we have considered, i.e. a Sauter pulse, we could calculate the first  $\mathcal{O}(50)$  orders of the  $\chi$  expansions without too much of a problem. This is not to say that we actually need that many terms. The method in [44] allows one to incorporate the leading  $\chi \gg 1$  scaling into the resummation in order to reduce the number of terms from the  $\chi \ll 1$  expansion needed to reach convergence for  $\chi = \mathcal{O}(1)$ . See also [45–47] for other methods to improve the convergence. We have not calculated the  $\chi \gg 1$  behavior of  $\mathbf{W}$ , so at this time we cannot make full use of these ideas. However, even by choosing (what is most likely) the wrong  $\chi \gg 1$  scaling for the method in [44], we have nevertheless managed to check that it agrees with the results obtained with the Padé-Borel method (in which we would not be able to incorporate the  $\chi \gg 1$  scaling even if we knew it). Comparing the results of these two different methods allows us to estimate the relative error of the resummations. Calculating the  $\chi \gg 1$  limit of  $\mathbf{W}$  would be very useful even if we are only interested in the numerical values of  $\mathbf{W}$  for  $\chi < 1$ . We leave this for future studies, since for the example we have considered there is no problem to calculate many orders in  $\chi \ll 1$ . The results are shown in Fig. 3. We see that a Padé resummation of the  $\alpha$  expansion requires less than ten terms to reach convergence. One can find an even faster convergence by using additional information about what the result is expected to be (see [26]), but a standard Padé resummation is good enough here. We also see that the resummed results converge to the results obtained by numerically solving the integro-differential equation without making any expansions. The fact that we only need a few terms from the  $\alpha$  expansion means that the resummation approach is in fact practical. Needless to say, having two very different methods for obtaining the same results is useful to be able to check the precision.

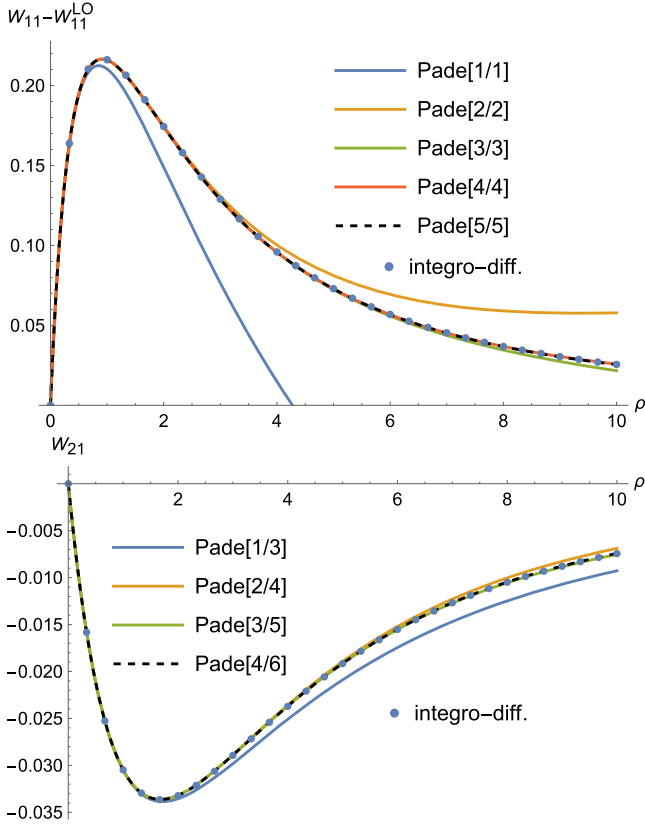


FIG. 3. The first moment,  $\mathbf{W}(m=1)$ , for a Sauter pulse and  $\chi_0 = 1/2$ . “Pade[ $i/j$ ]” means a Padé approximant of order [ $i/j$ ] has been used to resum the  $\alpha$  expansion.

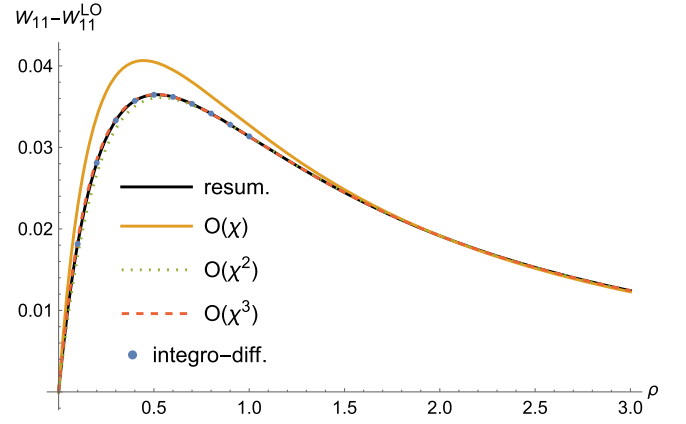


FIG. 4. Same as in Fig. 1 but for  $\chi_0 = 1/20$ .  $\mathcal{O}(\chi)$  is the leading order (18) [or (33)],  $\mathcal{O}(\chi^2)$  is obtained by also including the NLO (34), and  $\mathcal{O}(\chi^3)$  includes the NNLO.

### C. Higher moments and higher orders

In this section we consider higher moments  $m$  and the higher orders  $\mathcal{O}(\chi^2)$  and  $\mathcal{O}(\chi^3)$ . We first rescale  $\mathbf{w}$  in (11) as

$$\mathbf{w}_{m,k} = \frac{1}{\rho^{m+k}} \boldsymbol{\omega}_{m,k}. \quad (31)$$

Then the zeroth order (the classical LL result) is

$$\boldsymbol{\omega}_{m,0} = \frac{1}{y^m}, \quad (32)$$

where  $y$  is given by (15). The generalization of (17)–(19) to arbitrary moments is given by

$$\boldsymbol{\omega}_{m,1} = \int_{\sigma}^{\infty} d\varphi F^3(\varphi) \left\{ \frac{55}{32\sqrt{3}} \frac{d^2 \boldsymbol{\omega}_{m,0}}{dy^2} + \frac{1}{y-J(\varphi)} \begin{pmatrix} -\frac{55}{8\sqrt{3}} & \frac{3}{2} \\ \frac{3}{2} & -\frac{55}{8\sqrt{3}} \end{pmatrix} \cdot \frac{d\boldsymbol{\omega}_{m,0}}{dy} + \frac{1}{[y-J(\varphi)]^2} \frac{3}{2} \begin{pmatrix} 0 & 1 \\ 0 & -\frac{5\sqrt{3}}{8} \end{pmatrix} \cdot \boldsymbol{\omega}_{m,0} \right\}. \quad (33)$$

At  $\mathcal{O}(\chi^2)$  we find

$$\begin{aligned} \boldsymbol{\omega}_{m,2} = & \int_{\sigma}^{\infty} d\varphi F^3 \left\{ \frac{55}{32\sqrt{3}} \frac{d^2 \boldsymbol{\omega}_{m,1}}{dy^2} + \frac{1}{y-J} \begin{pmatrix} -\frac{55}{8\sqrt{3}} & \frac{3}{2} \\ \frac{3}{2} & -\frac{55}{8\sqrt{3}} \end{pmatrix} \cdot \frac{d\boldsymbol{\omega}_{m,1}}{dy} + \frac{1}{(y-J)^2} \frac{3}{2} \begin{pmatrix} 0 & 1 \\ 0 & -\frac{5\sqrt{3}}{8} \end{pmatrix} \cdot \boldsymbol{\omega}_{m,1} \right\} \\ & + \int_{\sigma}^{\infty} d\varphi F^4 \left\{ \frac{7}{6} \frac{d^3 \boldsymbol{\omega}_{m,0}}{dy^3} + \frac{1}{y-J} \begin{pmatrix} -7 & \frac{105\sqrt{3}}{64} \\ \frac{105\sqrt{3}}{64} & -7 \end{pmatrix} \cdot \frac{d^2 \boldsymbol{\omega}_{m,0}}{dy^2} \right. \\ & \left. + \frac{1}{(y-J)^2} \begin{pmatrix} 27 & -\frac{105\sqrt{3}}{16} \\ -\frac{315\sqrt{3}}{32} & 21 \end{pmatrix} \cdot \frac{d\boldsymbol{\omega}_{m,0}}{dy} + \frac{1}{(y-J)^3} \begin{pmatrix} 0 & -\frac{315\sqrt{3}}{32} \\ 0 & 18 \end{pmatrix} \cdot \boldsymbol{\omega}_{m,0} \right\}. \quad (34) \end{aligned}$$

We have also calculated a similar result for  $\mathcal{O}(\chi^3)$ . We compare the above result with a numerical computation of (23) in Fig. 4 for  $\chi_0 = 1/20$ . We see that if we only include  $\mathcal{O}(\chi)$ , then there is a noticeable difference from the exact

result, while including  $\mathcal{O}(\chi^2)$  gives a good agreement. Including also  $\mathcal{O}(\chi^3)$  gives a slight improvement, which is probably not experimentally relevant, but is sufficiently noticeable to provide a check of the third order as well as a

further check of the overall structure of this expansion. There is no problem to evaluate (34), but, at least for a Sauter pulse, we found that it is much faster to first make a double expansion in  $\chi \ll 1$  and  $\alpha$ , as in the double-resummation approach in Sec. II B, but keep the  $\chi \ll 1$  expansion un-resummed and only resum the  $\alpha$  expansion [with  $\rho = \mathcal{O}(\chi^0)$ ].

### III. MELLIN TRANSFORM

In this section we treat  $m$  as a Mellin integration variable. The goal is to obtain the momentum spectrum from the moments. Note that knowing only the first couple of moments,  $m = 0, 1, 2$ , does not allow us to deduce the shape of the distribution. For  $m \gg 1$ , only the first term in (33) and (34) contributes to leading order,

$$\omega_{m,k} \approx \frac{m^2}{y^2} \frac{55}{32\sqrt{3}} \int_{\sigma}^{\infty} d\varphi F^3 \omega_{m,k-1}, \quad (35)$$

for both  $k = 1$  and  $k = 2$ . It is natural to guess that this formula will continue to hold for arbitrary  $k$ . Then we have

$$\begin{aligned} \omega_{m,k} &\approx \frac{\mathbf{1}}{y^m} \left( \frac{m^2}{y^2} \frac{55}{32\sqrt{3}} \right)^k \int_{\sigma}^{\infty} d\varphi_k F^3(\varphi_k) \\ &\quad \times \int_{\varphi_k}^{\infty} d\varphi_{k-1} F^3(\varphi_{k-1}) \dots \int_{\varphi_2}^{\infty} d\varphi_1 F^3(\varphi_1) \\ &= \frac{\mathbf{1}}{y^m} \frac{1}{k!} \left( \frac{m^2}{y^2} \frac{55}{32\sqrt{3}} \int_{\sigma}^{\infty} d\varphi F^3 \right)^k. \end{aligned} \quad (36)$$

Summing over all orders in  $\chi_0$  gives

$$\mathbf{W} \approx \frac{\mathbf{1}}{(1 + \rho J)^m} \exp \left\{ \frac{\chi_0 \lambda}{4} (1 + \rho J)^2 m^2 \right\}, \quad (37)$$

where

$$\lambda = \frac{55\rho}{8\sqrt{3}[1 + \rho J(\sigma)]^4} \int_{\sigma}^{\infty} d\sigma' F^3(\sigma'). \quad (38)$$

The reason for defining  $\lambda$  like this will be explained in a moment.

Although we obtained (37) by summing over all orders in a  $\chi_0 \ll 1$  expansion, it is better to think of the result as the leading order in a  $\chi_0 \ll 1$  expansion where both  $\rho = \mathcal{O}(1)$  and  $\chi_0 m^2 = \mathcal{O}(1)$ . We will now rederive (37) [and hence confirm that (35) holds for all  $k$ ] by assuming  $\chi_0 m^2 = \mathcal{O}(1)$  right from the start. We start with the ansatz

$$\mathbf{W} = \frac{\mathbf{1}}{(1 + \rho J)^m} \sum_{k=0}^{\infty} \bar{\mathbf{w}}_k(\sigma, \rho, \mu) \chi_0^{k/2}, \quad (39)$$

where  $\mu = m\sqrt{\chi_0}$ . The zeroth-order term in (39) will turn out to be the same as (37), but with this approach we can

now also calculate higher orders. Note that the expansion is in powers of  $\chi_0^{1/2}$  rather than  $\chi_0$ , so one can expect higher orders to be numerically important for moderately small values of  $\chi_0$ . We plug this ansatz into (7), multiply both sides by  $(1 + \rho J)^m$ , change variable from  $q = \chi\gamma/(1 + \chi\gamma)$  to  $\gamma$  (same as before), and then expand the integrand in powers of  $\sqrt{\chi_0}$  with  $\rho = \mathcal{O}(1)$  and  $\mu = \mathcal{O}(1)$ . In the term proportional to  $\mathbf{M}_C$ , we have  $\bar{\mathbf{w}}_k(\sigma, [1 - q]\rho, \sqrt{1 - q}\mu)$ , which, after expanding in  $\chi_0 \ll 1$ , gives terms with derivatives of  $\bar{\mathbf{w}}$  with respect to  $\rho$  and  $\mu$ . The expansion of (7) starts at  $\mathcal{O}(1/\sqrt{\chi_0})$ , but both sides are automatically equal at this order. At  $\mathcal{O}(\chi_0^0)$ , we find

$$\partial_{\sigma} \bar{\mathbf{w}}_0 - \rho^2 F^2 \partial_{\rho} \bar{\mathbf{w}}_0 - \frac{\mu\rho}{2} F^2 \partial_{\mu} \bar{\mathbf{w}}_0 = -\frac{55\mu^2 \rho F^3}{32\sqrt{3}(1 + \rho J)^2} \bar{\mathbf{w}}_0. \quad (40)$$

We again solve this equation by changing variable from  $\rho$  to  $y$  as in (15). We find

$$\bar{\mathbf{w}}_0 = \mathbf{1} \exp \left\{ \mu^2 \frac{55}{32\sqrt{3}} \frac{y - J(\sigma)}{y^2} \int_{\sigma}^{\infty} F^3 \right\}, \quad (41)$$

which is the same as in (37).

At  $\mathcal{O}(\chi^{1/2})$  we find an equation which is solved by

$$\bar{\mathbf{w}}_1 = \bar{\mathbf{w}}_0 \cdot \left( \frac{\mu}{\rho} \mathbf{H}_1^{(1)} + \frac{\mu^3}{\rho^2} \mathbf{H}_3^{(1)} \right), \quad (42)$$

where

$$\begin{aligned} \mathbf{H}_1^{(1)} &= \int_{\sigma}^{\infty} d\varphi \left\{ \frac{55F^3(\varphi)[5y - J(\varphi)]}{32\sqrt{3}y^2[y - J(\varphi)]} \begin{pmatrix} 1 & 0 \\ 0 & 1 \end{pmatrix} \right. \\ &\quad \left. - \frac{3F^3(\varphi)}{2y[y - J(\varphi)]} \begin{pmatrix} 0 & 1 \\ 1 & 0 \end{pmatrix} \right\} \end{aligned} \quad (43)$$

and

$$\mathbf{H}_3^{(1)} = \int_{\sigma}^{\infty} d\varphi \left\{ \frac{7F^4(\varphi)}{6y^3} - \frac{55^2 F^3(\varphi)}{2^8 3y^4} \int_{\varphi}^{\infty} F^3 \right\} \begin{pmatrix} 1 & 0 \\ 0 & 1 \end{pmatrix}. \quad (44)$$

At  $\mathcal{O}(\chi)$  we find

$$\bar{\mathbf{w}}_2 = \bar{\mathbf{w}}_0 \cdot \left( \frac{1}{\rho} \mathbf{H}_0^{(2)} + \frac{\mu^2}{\rho^2} \mathbf{H}_2^{(2)} + \frac{\mu^4}{\rho^3} \mathbf{H}_4^{(2)} + \frac{\mu^6}{\rho^4} \mathbf{H}_6^{(2)} \right), \quad (45)$$

where  $\mathbf{H}_j^{(2)}$  depend on  $\sigma$  and  $y$  but not on  $\mu$ . With this ansatz for the dependence on  $\mu$  the equations for  $\mathbf{H}_j^{(2)}$  are easy to solve. For example,

$$\begin{aligned} \partial_\sigma(\mathbf{H}_2^{(2)})_{1,1} &= \frac{7F^4(3y-J)}{2y^3(y-J)} - \frac{3025F^3(7y-3J)}{1536y^4(y-J)} \int_\sigma^\infty F^3 \\ &\quad - \frac{55F^3(5y-J)}{32\sqrt{3}y^2(y-J)} (\mathbf{H}_1^{(1)})_{1,1} + \frac{3F^3}{2y(y-J)} (\mathbf{H}_1^{(1)})_{2,1} \\ &\quad + \frac{55F^3}{16\sqrt{3}y} \partial_y (\mathbf{H}_1^{(1)})_{1,1}, \end{aligned} \quad (46)$$

where  $(\cdot)_{i,j}$  indicates components of the matrices and the argument  $\sigma$  for  $F$ ,  $J$ , and  $\mathbf{H}$  is left implicit. It is straightforward to solve these equations, but the resulting expressions for  $\mathbf{H}_j^{(2)}$  are not particularly illuminating.

Note that it was not necessary to assume that the moment order  $m$  is an integer. In our approach, the equation for  $\mathbf{W}(m)$  does not depend on other values of  $m$ .  $m$  is just a parameter, and there is no problem to consider it to be an arbitrary continuous variable. In fact, in the following we will consider complex  $m$  in order to perform an inverse Mellin transform. Note that (7) allows us to find the moments without having to consider the spectrum  $\mathbf{S}$ , but if we have calculated  $\mathbf{S}$ , then we can obtain the same moments from

$$\mathbf{W}(m) = \int_{-\infty}^1 dx (1-x)^m \mathbf{S} = \int_0^\infty dv v^m \mathbf{S}, \quad (47)$$

where we have changed variable from  $x$  to  $v = 1 - x$ . By letting  $m$  be a continuous, complex parameter, this gives the Mellin transform of the spectrum. We can therefore obtain the spectrum from the moments by performing an inverse Mellin transform,

$$\mathbf{S} = \frac{1}{v} \int_{-i\infty}^{i\infty} \frac{dm}{2\pi i} v^{-m} \mathbf{W}(m). \quad (48)$$

We can obtain a  $\chi_0 \ll 1$  expansion of  $\mathbf{S}$  by plugging in the expansion in (39),

$$\begin{aligned} \mathbf{S} &= \frac{1}{v\sqrt{\chi_0}} \int \frac{d\mu}{2\pi i} e^{a\mu^2 - \mu L} \\ &\quad \times \left( 1 + \sqrt{\chi_0} \left[ \frac{\mu}{\rho} \mathbf{H}_1^{(1)} + \frac{\mu^3}{\rho^2} \mathbf{H}_3^{(1)} \right] + \chi_0 [\dots] + \dots \right), \end{aligned} \quad (49)$$

where  $a > 0$  is the coefficient of  $\mu^2$  in the exponent of (41) and

$$L = \frac{1}{\sqrt{\chi_0}} \ln[(1 + \rho J)v]. \quad (50)$$

To perform the complex moment integral in (49), we change variable from

$$\mu = \frac{L}{2a} + \frac{i}{\sqrt{a}} \nu \quad (51)$$

to  $\nu$  and integrate along the real axis, which corresponds to a contour parallel to the imaginary axis in the complex  $m$  plane. As explained in [29], it is natural to consider

$$X = \frac{1}{\sqrt{\lambda\chi_0}} \left( \frac{1}{1 + \rho J} - v \right) \quad (52)$$

as an  $\mathcal{O}(\chi^0)$  variable for the spectrum, because if one makes a plot of the spectrum with  $X$  on the  $x$  axis, with the length of the plotted interval being roughly  $\mathcal{O}(10)$ , then one can see the entire peak and the peak is not just a sharp needle, even if one makes  $\chi_0$  arbitrarily small. This means, in particular,

$$L = -\sqrt{\lambda}(1 + \rho J)X + \mathcal{O}(\sqrt{\chi_0}). \quad (53)$$

Thus, after performing the Gaussian integrals, we expand the result in powers of  $\chi_0$  with  $X$  rather than  $v$  (or  $x$ ) as  $\mathcal{O}(\chi^0)$ . We find

$$\begin{aligned} \mathbf{S} &= \frac{e^{-X^2}}{\sqrt{\pi\lambda\chi_0}} \left\{ \mathbf{1} + \frac{\sqrt{\chi_0}X}{\sqrt{\lambda}} \left[ \lambda(1-X^2)(1 + \rho J)\mathbf{1} \right. \right. \\ &\quad \left. \left. - \frac{2\mathbf{H}_1^{(1)}}{\rho(1 + \rho J)} + \frac{12 - 8X^2}{\lambda\rho^2(1 + \rho J)^3} \mathbf{H}_3^{(1)} \right] + \mathcal{O}(\chi_0) \right\}. \end{aligned} \quad (54)$$

Note that, with  $X = \mathcal{O}(1)$ , the expansion is in powers of  $\sqrt{\chi_0}$  rather than  $\chi_0$ . For a constant field we can compare with the results in [29], which we obtained there with a very different approach. We can immediately see that the leading order is the same. The  $\mathcal{O}(\sqrt{\chi_0})$  term agrees with Eqs. (111) and (112) in [29]. We have also checked that the  $\mathcal{O}(\chi_0)$  term agrees with the corresponding constant field result, which was used for plots in [29] but not explicitly shown. We explain how to obtain the spectrum for a nonconstant field with the same approach as in [29] in Appendix B.

One could also perform the inverse Mellin transform numerically. If one still makes the change of variable in (51), then the integrand behaves roughly as  $e^{-\nu^2}$  close to  $\nu = 0$ . Since  $e^{-4^2} = \mathcal{O}(10^{-7})$ , one could expect to find a good precision by integrating from  $\nu = -4$  to  $\nu = 4$ . One could then choose a set of points in this interval, solve (7) at each of these points, and then make an interpolation function for  $\mathbf{W}(\nu)$ . However, we leave that for future studies.

#### IV. MAXIMUM ENTROPY

In Sec. III we showed how to obtain the spectrum by treating the moment order  $m$  as a Mellin variable, and then integrating over  $m$  in the complex plane. In this section we will show another way, where we obtain the spectrum from a handful of moments by using the principle of maximum entropy [48–50]. This approach does not rely on a  $\chi \ll 1$  expansion (but we still have in mind values of  $\chi$  for which

pair production can be neglected). The idea is to approximate the true spectrum  $S_{11} = \mathbf{e}_0 \cdot \mathbf{S} \cdot \mathbf{e}_0$  (we average and sum over the initial and final spins for simplicity) with a distribution  $S_N$  which maximizes the entropy [48,49]

$$-\int dx S(x) \ln \frac{S(x)}{p(x)} \quad (55)$$

subject to the constraints on the moments,

$$\int dx (1-x)^m S_N \stackrel{!}{=} \mathbf{e}_0 \cdot \mathbf{W}(m) \cdot \mathbf{e}_0 \quad (56)$$

for  $m = 0, 1, 2, \dots, N$ . The function that satisfies these constraints and maximizes the entropy is given by [48–50]

$$S_N = p(x) \exp \left\{ - \sum_{n=0}^N \lambda_n x^n \right\}, \quad (57)$$

where  $\lambda_n$  are constants determined by (56). For the case we focus on here we expect  $S(x)$  to be not too different from a Gaussian, and we therefore choose the prior distribution [49]  $p(x) = 1$  [choosing  $p(x) = a \exp[-c(x-b)^2]$  with some constants  $a$ ,  $b$ , and  $c$  gives the same result as it just corresponds to a shift in  $\lambda_0$ ,  $\lambda_1$ , and  $\lambda_2$ ]. In Fig. 5, we compare the results with the exact numerical result obtained in [29] for a constant field. At  $N = 5$  or  $N = 6$  we have a good agreement. This is good news because each moment only takes a couple of minutes to compute, and solving (56) is also very fast. So this maximum-entropy approach is much faster than a direct computation of the spectrum as in [29].

The principle of maximum entropy alone does not imply that having a polynomial in the exponent (57) is necessarily

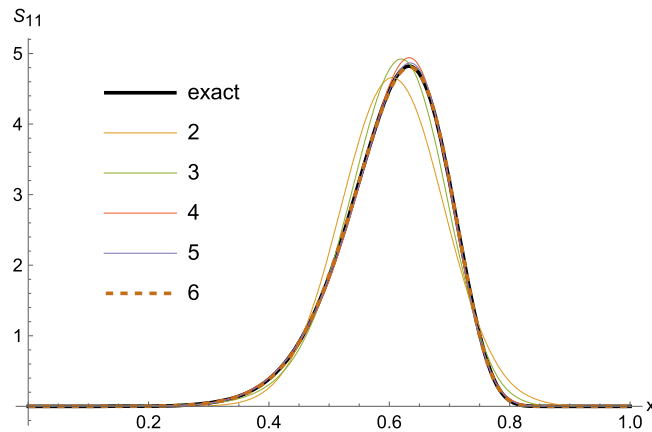


FIG. 5. The spectrum  $S_{11} = \mathbf{e}_0 \cdot \mathbf{S} \cdot \mathbf{e}_0$  for a constant field with  $\chi = 0.1$  and  $u := (2/3)\chi\alpha\alpha_0\Delta\phi = 2$ . The black line shows the numerical result obtained in [29] by solving directly the equation for the spectrum (or rather the cumulative function, which is then differentiated). The other lines show the maximum-entropy distribution  $S_N$  in (57) with  $N = 2, 3, \dots, 6$ .

the best way to approximate the spectrum. There is a polynomial in the exponent simply because we have chosen to impose the constraints (56) for integer moments. If one instead chooses a set of fractional [51] or negative [52] powers  $m$  (or the expectation value of some more nontrivial function), then one has a sum of such terms in the exponent. So, one can try to figure out what sort of  $x$  dependence to expect and then let that guide the choice of  $m$ 's in order to find convergence with even fewer  $m$ 's. Note again that in our approach there is no problem to obtain noninteger moments, because each moment is obtained without considering any other moments. We leave such investigations for the future and instead consider the following approach.

The maximum entropy is expected to give the best estimate given a set of moments but assuming no other information. However, in our case we do have some additional information provided by the  $\chi \ll 1$  expansion in (B4). We consider again a constant field. The results for  $\rho_1$  up to  $\rho_5$  were calculated for [29], but only  $\rho_1$  was explicitly presented. What is relevant here is the analytical structure of these functions,

$$\begin{aligned} \rho_1(u, X) &= \sum_{n=0}^1 \rho_{1,2n+1}(u) X^{2n+1}, \\ \rho_2(u, X) &= \sum_{n=0}^3 \rho_{2,2n}(u) X^{2n}, \\ \rho_3(u, X) &= \sum_{n=0}^4 \rho_{1,2n+1}(u) X^{2n+1}, \\ \rho_4(u, X) &= \sum_{n=0}^6 \rho_{1,2n}(u) X^{2n}, \\ \rho_5(u, X) &= \sum_{n=0}^7 \rho_{1,2n+1}(u) X^{2n+1}. \end{aligned} \quad (58)$$

If we just exponentiate these terms,

$$\begin{aligned} &\mathbf{e}_0 \cdot \sum_{n=0}^5 \rho_n(u, X) \chi^{n/2} \cdot \mathbf{e}_0 \\ &=: \exp \left\{ \sum_{n=1}^5 E_n(u, X) \chi^{n/2} \right\} + \mathcal{O}(\chi^{6/2}), \end{aligned} \quad (59)$$

where the coefficients  $E_n$  are defined by taking the logarithm of the left-hand side and expanding to  $\mathcal{O}(\chi^{5/2})$ , then we find that  $E_1$  contains terms proportional to either  $X$  or  $X^3$ ;  $E_2$  contains  $X^0$ ,  $X^2$ , and  $X^4$ ;  $E_3$  contains odd powers from  $X$  to  $X^5$ ;  $E_4$  contains even powers from  $X^0$  to  $X^6$ ; and  $E_5$  contains odd powers from  $X$  to  $X^7$ . Thus, if  $N(\cdot)$  counts the number of terms in the  $X$  polynomial,

$$N(\rho_1, \rho_2, \rho_3, \rho_4, \rho_5) = (2, 4, 5, 7, 8) \quad (60)$$

while

$$N(E_1, E_2, E_3, E_4, E_5) = (2, 3, 3, 4, 4). \quad (61)$$

We see that, at the very least, the information stored in  $(\rho_1, \rho_2, \rho_3, \rho_4, \rho_5)$  can be more compactly stored in  $(E_1, E_2, E_3, E_4, E_5)$ . We can make it even a bit more compact in terms of  $R_n$  defined by

$$\begin{aligned} & \frac{e^{-X^2}}{\sqrt{\pi}} \mathbf{e}_0 \cdot \sum_{n=0}^5 \boldsymbol{\rho}_n(u, X) \chi^{n/2} \cdot \mathbf{e}_0 \\ & =: \frac{1}{2} \frac{\partial}{\partial X} \operatorname{erf} \left\{ X + \sum_{n=1}^5 R_n(u, X) \chi^{n/2} \right\} + \mathcal{O}(\chi^{6/2}). \end{aligned} \quad (62)$$

The inspiration for this ansatz has nothing to do with the maximum entropy principle. Instead it comes from noting that the  $\chi \ll 1$  expansion of the cumulative function can be expressed as

$$\begin{aligned} \mathbf{M} &= \frac{1}{2} (1 + \operatorname{erf}(X)) \mathbf{1} - \frac{e^{-X^2}}{\sqrt{\pi}} \sum_{n=1}^{\infty} \mathbf{h}_n(u, \chi) H_{n-1}(X) \\ &= \sum_{n=0}^{\infty} \mathbf{h}_n(u, \chi) \left( -\frac{d}{dX} \right)^n \frac{1}{2} (1 + \operatorname{erf}(X)), \end{aligned} \quad (63)$$

where  $H$  are Hermite polynomials and  $\mathbf{h}_0 = \mathbf{1}$ , suggesting that one interpret it as the Taylor expansion of  $\operatorname{erf}(X + \dots)$ . The actual justification for (62) is that it does indeed lead to a more compact result,

$$N(R_1, R_2, R_3, R_4, R_5) = (2, 2, 3, 3, 4). \quad (64)$$

In (59) we have the exponential of a polynomial in  $x$ , but it is not a proof of (57). In (59) there are no undetermined quantities; i.e. one can evaluate it without matching with (56). However, Eq. (59) is not a replacement of (57) either, because (59) only provides a partial resummation of the  $\chi \ll 1$  series. To obtain a full resummation one would need to resum  $\sum E_n \chi^{n/2}$ . Equation (62), too, only gives a partial resummation. Thus, if  $\chi$  is small but not very small, one can expect the  $\chi \ll 1$  expansions to break down regardless of whether one uses the expansion in terms of  $\boldsymbol{\rho}_n$ ,  $E_n$ , or  $R_n$ . We instead take (59) as motivation for choosing the prior distribution [49] such that we have (57) with  $p(x) = 1$ .

Similarly, we have also taken (62) as motivation for matching the moments onto

$$M_N = \frac{1}{2} \left[ 1 + \operatorname{erf} \left( \sum_{n=0}^{N-1} \kappa_n \chi^n \right) \right], \quad (65)$$

where the coefficients  $\kappa_n$  are obtained by

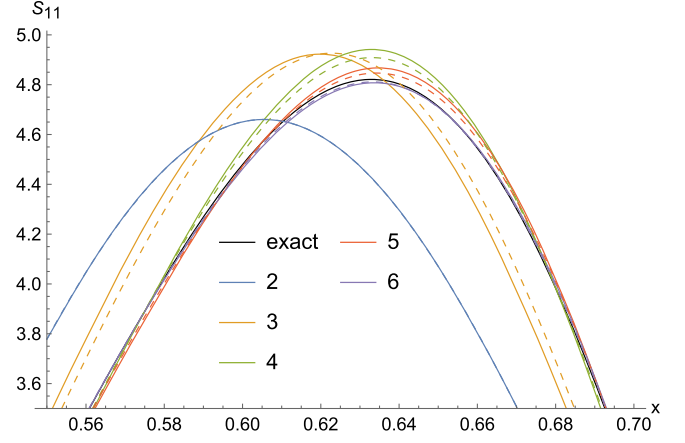


FIG. 6. The solid lines are the same as in Fig. 5, and the dashed lines show (65). The solid and dashed lines for  $N = 2$  coincide.

$$\int_0^1 dx m (1-x)^{m-1} M_N \stackrel{!}{=} \mathbf{e}_0 \cdot \mathbf{W}(m) \cdot \mathbf{e}_0. \quad (66)$$

This provides an alternative to the maximum-entropy fit (57). Equations (57) and (65), obtained using the same set of moments, are compared in Fig. 6. We see that (65) provides a slight improvement compared to (57). More importantly, having two different ways of obtaining the spectrum from the moments allows us to estimate the error in other cases when we do not already have the exact spectrum.

In Fig. 5 we have chosen  $u$  sufficiently large so that the peak is well separated from  $x = 0$ . As seen in Fig. 1 or 3 in [29], for small  $u$  we instead have a sharp peak at  $x = 0$ , which does not look like a Gaussian even to a first approximation. After trying to anyway use (57) with  $p(x) = 1$  for one such example, it looks like one can see that there is a peak at  $x = 0$ , but the convergence is much slower. So, even if we did not have access to the exact spectrum, we would be able to tell that (57) with  $p(x) = 1$  is not as good in this case. This suggests that one should try to find another prior distribution  $p(x)$  which captures the sharp peak to some rough first approximation, and/or choose to match with different moments. We leave that for future studies.

## V. BEYOND LCF

In this section we will generalize the results in Sec. II beyond the LCF regime. The incoherent-product approximation is still valid even if  $a_0$  is not large, provided the pulse is long enough.

We begin by noting that the longitudinal-momentum fraction is small,  $q = kl/kp = \mathcal{O}(b_0)$ , where  $l$  is the photon momentum. We can therefore Taylor expand the moments

$$\tilde{\mathbf{M}}([1-q]b_0) \approx \tilde{\mathbf{M}}(b_0) - qb_0 \frac{\partial \tilde{\mathbf{M}}}{\partial b_0} + (qb_0)^2 \frac{\partial^2 \tilde{\mathbf{M}}}{\partial b_0^2}. \quad (67)$$

Although  $b_0 \ll 1$ , we cannot expand  $\tilde{\mathbf{M}}(b_0)$  since  $b_0$  appears in  $\rho = \mathcal{O}(1)$ . We plug this expansion into (2), change variable to  $\gamma = r/b_0$  as in (12), expand the integrand [but not  $\tilde{\mathbf{M}}(b_0)$ ] in  $b_0 \ll 1$  with  $\gamma$  and  $\theta$  independent of  $b_0$ , and perform the resulting  $\gamma$  integrals. Since we now consider more general regimes,  $\mathbf{M}_{L,C}$  can in general not be expressed in terms of either Airy functions (for LCF) or Bessel functions (for LMF). Instead we have  $\theta$  integrals as in (A1) (see [24] for the other components of  $\mathbf{M}_C$  for photon polarization). The definitions of  $\mathbf{R}$ ,  $\mathbf{V}$ , etc., below can be found in Appendix A. In the derivation of the Mueller matrices, two light-front-time variables appear as  $\sigma = (\phi_2 + \phi_1)/2$  and  $\theta = \phi_2 - \phi_1$ , where  $\phi_{1,2}$  are light-front-time variables for the amplitude and its complex conjugate. In the LCF regime we have  $\theta = \mathcal{O}(1/a_0)$ , so then when expanding in  $1/a_0 \ll 1$  the probabilities localizes, i.e. can be expressed in terms of the field and its first derivatives evaluated at  $\theta = 0$ . Thus, in the results below where the  $\theta$  integrals receive significant contributions for regions where  $\theta$  is not small, we have clear nonlocal, beyond-LCF effects.

Performing the longitudinal-momentum ( $\gamma$ ) integral before the  $\theta$  integral gives

$$\int_0^\infty d\gamma \gamma^n \exp\left(\frac{i}{2}\Theta\gamma\right) = n! \left(-\frac{i}{2}\Theta\right)^{-1-n}, \quad (68)$$

where  $\Theta = \theta M^2$  and  $M^2(\theta, \sigma)$  is the effective mass [53]. The resulting  $\theta$  integrals are now either symmetric or antisymmetric in  $\theta$ . In the antisymmetric case the  $\theta$  integral is equal to  $-i\pi$  times the residue at  $\theta = 0$  (the  $\theta$  contour goes above the pole at  $\theta = 0$ ), which means that the probability localizes even though there is no small or large parameter that forces it to be so. Some terms will therefore be local even beyond the LCF regime. But for terms with symmetric  $\theta$  integrals, we obtain in general nonlocal results.

We consider first the matrix multiplying  $\tilde{\mathbf{M}}(b_0)$  in (67),

$$\left[ \int_0^1 dq (\mathbf{M}_L + \mathbf{M}_C) \right] \cdot \tilde{\mathbf{M}}(b_0) =: \mathbf{m}_0 \cdot \tilde{\mathbf{M}}. \quad (69)$$

Unitarity ensures that some of the components in the above sum cancel,

$$\mathbf{R}_L + \mathbf{R}_C = \begin{pmatrix} 0 & \mathbf{R}_1^C - \mathbf{R}_0^C \\ 0 & \mathbf{R}_{01}^C - \langle \mathbb{R}^C \rangle \mathbf{1} + \mathbf{R}_{01}^{\text{rot}} \end{pmatrix}. \quad (70)$$

We have

$$\mathbf{R}_1^C - \mathbf{R}_0^C = \frac{q^2}{s} \mathbf{V}, \quad (71)$$

and using (68) with  $n = 2$ , we find

$$\mathbf{e}_0 \cdot \mathbf{m}_0 = \frac{8ab_0^2}{\pi} \int d\theta \frac{\mathbf{V}}{\theta \Theta^3}. \quad (72)$$

The integrand is odd since  $\Theta(-\theta) = -\Theta(\theta)$  and  $\mathbf{V}(-\theta) = -\mathbf{V}(\theta)$ , so, if we integrate along the real axis from  $-\infty$  to  $-\epsilon < 0$ , then clockwise around a semicircle to  $+\epsilon$ , and finally along the real axis from  $\epsilon$  to  $+\infty$ , the two contributions from the real axis cancel, and in the limit  $\epsilon \rightarrow 0$  we are left with  $-i\pi$  times the residue at  $\theta = 0$ . We find

$$\mathbf{e}_0 \cdot \mathbf{m}_0 = ab_0^2 i \sigma_2 \cdot \left[ \mathbf{a}^2 \mathbf{a}' - \frac{1}{6} \mathbf{a}''' \right], \quad (73)$$

where we have a frame where  $\mathbf{a} = a_1 \mathbf{e}_1 + a_2 \mathbf{e}_2$ ,

$$\sigma_2 = i(\mathbf{e}_2 \mathbf{e}_1 - \mathbf{e}_1 \mathbf{e}_2) \quad (74)$$

is one of the Pauli matrices, and the field is evaluated at  $\sigma$ , so this is a local term. If the field is linearly polarized with the electric field along the  $x$  axis,  $\mathbf{a} \propto \mathbf{e}_1$ , then  $\mathbf{e}_0 \cdot \mathbf{m}_0 \propto \mathbf{e}_2$  is parallel or antiparallel to the magnetic field.

Next we consider the diagonal terms in  $\mathbf{m}_0$ , which come from the diagonal terms of  $\mathbf{R}_{01}^C - \langle \mathbb{R}^C \rangle \mathbf{1}$  in (70). Using again (68) with  $n = 2$  gives

$$\mathbf{m}_0|_{\text{diag}} = \frac{2}{\pi} ab_0^2 \int \frac{d\theta}{\theta \Theta^3} (\Delta a^2 [\mathbf{e}_1 \mathbf{e}_1 + \mathbf{e}_2 \mathbf{e}_2] - 4\mathbf{e}_3 \mathbf{e}_3), \quad (75)$$

where

$$\Delta a^2 = \left[ \mathbf{a} \left( \sigma + \frac{\theta}{2} \right) - \mathbf{a} \left( \sigma - \frac{\theta}{2} \right) \right]^2. \quad (76)$$

For this term we have a symmetric  $\theta$  integrand, so the integral is not simply given by the residue at  $\theta = 0$ . This is therefore a nonlocal term.

$\mathbf{m}_0$  also contains off-diagonal terms due to  $\mathbf{R}_{01}^C$  and  $\mathbf{R}_{01}^{\text{rot}}$  in (70). For a linearly polarized field,  $\mathbf{a} \propto \mathbf{e}_1$ , these off-diagonal terms are proportional to  $\mathbf{e}_1 \mathbf{e}_3$  or  $\mathbf{e}_3 \mathbf{e}_1$  and make the spin components in the  $\hat{\mathbf{E}}\text{-}\hat{\mathbf{k}}$  plane ( $\mathbf{e}_1\text{-}\mathbf{e}_3$  plane) rotate. We do not need to consider these terms if we consider initial and final spins along the magnetic field direction. For a symmetrically oscillating field with circular polarization those off-diagonal terms average out, and we are instead left with a term proportional to  $\sigma_2$ , which leads to spin rotation in the plane perpendicular to the propagation direction  $\hat{\mathbf{k}} = \mathbf{e}_3$ . In this case we can omit this off-diagonal term by considering initial and final spin parallel to  $\hat{\mathbf{k}}$ . We will explain one way of dealing with fast spin rotation in Sec. VI. For now, we consider spin components that do not rotate.

We turn to the matrices,  $\mathbf{m}_1$  and  $\mathbf{m}_2$ , which multiply  $\partial_{b_0} \tilde{\mathbf{M}}$  and  $\partial_{b_0}^2 \tilde{\mathbf{M}}$  in (67). Only  $\mathbf{M}_C$  contributes to these terms since they come from expanding the second term in (2).

For the diagonal elements we find for the leading and next-to-leading order

$$\mathbf{m}_1|_{\text{diag}} = \frac{2}{3}\alpha b_0 \mathbf{a}^2 \mathbf{1}_4 + \frac{12}{\pi} \alpha b_0^2 \mathbf{1}_4 \int \frac{d\theta}{\theta \Theta^3} [2 + \Delta a^2] \quad (77)$$

and

$$\mathbf{m}_2|_{\text{diag}} = -\frac{4}{\pi} \alpha b_0^2 \mathbf{1}_4 \int \frac{d\theta}{\theta \Theta^3} [2 + \Delta a^2], \quad (78)$$

where  $\mathbf{1}_4 = \sum_{j=0}^3 \mathbf{e}_j \mathbf{e}_j$ .

As for  $\mathbf{m}_0$ , we can again omit the off-diagonal terms proportional to  $\mathbf{e}_i \mathbf{e}_j$  if we consider spin components that do not rotate. The off-diagonal terms proportional to  $\mathbf{e}_0 \mathbf{e}_i$  and  $\mathbf{e}_i \mathbf{e}_0$ , though, cannot be omitted. We find

$$\mathbf{e}_0 \cdot \mathbf{m}_1 = \mathbf{m}_1 \cdot \mathbf{e}_0 = \mathbf{e}_0 \cdot \mathbf{m}_0 + \frac{2}{3} \alpha b_0^2 [a'_1 a''_1 - a'_2 a''_2] \hat{\mathbf{k}}, \quad (79)$$

where  $\mathbf{e}_0 \cdot \mathbf{m}_0$  is given by (73).  $\mathbf{e}_0 \cdot \mathbf{m}_2$  and  $\mathbf{m}_2 \cdot \mathbf{e}_0$  are higher order in  $b_0$ .

Only the first term in (77) contributes to leading order,

$$\partial_\sigma \tilde{\mathbf{M}}_0 = m_1^{\text{LO}} b_0 \partial_{b_0} \tilde{\mathbf{M}}_0, \quad (80)$$

where

$$\mathbf{m}_1^{\text{LO}} = \frac{2}{3} \alpha b_0 \mathbf{a}^2 \mathbf{1}_4 = m_1^{\text{LO}} \mathbf{1}_4. \quad (81)$$

The solution is given by the solution to LL, to the power of the moment,

$$\tilde{\mathbf{M}}_0 = \mathbf{1}_4 \left( \frac{1}{b_0} + \frac{2}{3} \alpha \int_\sigma^\infty \mathbf{a}^2 \right)^{-m}, \quad (82)$$

which agrees with (13).

For the next-to-leading order we have

$$\begin{aligned} \partial_\sigma \tilde{\mathbf{M}}_1 - m_1^{\text{LO}} b_0 \partial_{b_0} \tilde{\mathbf{M}}_1 \\ = - \left( \mathbf{m}_0 - [\mathbf{m}_1 - \mathbf{m}_1^{\text{LO}}] b_0 \partial_{b_0} + \mathbf{m}_2 \frac{b_0^2}{2} \partial_{b_0}^2 \right) \cdot \tilde{\mathbf{M}}_0 \\ =: -\rho \chi_0 \left( \mathbf{n}_0 + \mathbf{n}_1 b_0 \partial_{b_0} + \mathbf{n}_2 \frac{b_0^2}{2} \partial_{b_0}^2 \right) \cdot \tilde{\mathbf{M}}_0. \end{aligned} \quad (83)$$

Note that the  $\mathbf{n}_i$  matrices do not depend on  $b_0$ . We can solve (83) using the method of characteristics as before. With the notation in (11), (15), (31), and (32), we find

$$\boldsymbol{\omega}_1 = \int_\sigma^\infty d\varphi \left\{ \frac{\mathbf{n}_2}{2} \partial_y^2 + \frac{\mathbf{n}_2 - \mathbf{n}_1}{y - J} \partial_y + \frac{\mathbf{n}_0}{[y - J]^2} \right\} \cdot \boldsymbol{\omega}_0, \quad (84)$$

where  $\mathbf{n}_j$  and  $J$  are evaluated at  $\varphi$ , while  $Y = \frac{1}{\rho} + J(\sigma)$ . Equation (84) gives the first-order quantum correction

beyond the LCF regime. Below we will analyze its nonlocal structure, calculate its LCF ( $a_0 \gg 1$ ) and perturbative ( $a_0 \ll 1$ ) limits, and simplify it in the locally monochromatic-field regime, for both circular and linearly polarized fields.

We can express the nonlocal integrals above in terms of the following two functions:

$$\mathcal{H} = -\frac{4}{\pi a_0^2} \int \frac{d\theta}{\theta \Theta^3} (2 + \Delta a^2) \quad (85)$$

and

$$\mathcal{B} = -\frac{2}{\pi a_0^2} \int \frac{d\theta}{\theta \Theta^3} \Delta a^2. \quad (86)$$

From (78) we find

$$\mathbf{n}_2 = \frac{3\mathcal{H}}{2a_0} \mathbf{1}_4. \quad (87)$$

From (77) and (79) we find

$$\mathbf{n}_1 = 3\mathbf{n}_2 - \left\{ \frac{\mathbf{e}_0}{a_0^3}, \frac{3}{2} i\boldsymbol{\sigma}_2 \cdot \left[ \mathbf{a}^2 \mathbf{a}' - \frac{\mathbf{a}'''}{6} \right] + [\mathbf{a}' \cdot i\boldsymbol{\sigma}_2 \cdot \mathbf{a}''] \hat{\mathbf{k}} \right\}, \quad (88)$$

where  $\{\mathbf{e}_0, \mathbf{e}_i\} := \mathbf{e}_0 \mathbf{e}_i + \mathbf{e}_i \mathbf{e}_0$ . And from (75) and (73) we find

$$\begin{aligned} \mathbf{n}_0 = -\frac{3\mathcal{B}}{2a_0} (\mathbf{e}_1 \mathbf{e}_1 + \mathbf{e}_2 \mathbf{e}_2) + \frac{3}{2a_0} [\mathcal{H} - 2\mathcal{B}] \mathbf{e}_3 \mathbf{e}_3 \\ + \frac{3}{2a_0^3} \mathbf{e}_0 i\boldsymbol{\sigma}_2 \cdot \left[ \mathbf{a}^2 \mathbf{a}' - \frac{\mathbf{a}'''}{6} \right]. \end{aligned} \quad (89)$$

For unpolarized initial and final states we find, from (84),

$$\begin{aligned} \mathbf{e}_0 \cdot \mathbf{w}_{m,1} \cdot \mathbf{e}_0 = \frac{3m\rho}{4a_0 [1 + \rho J(\sigma)]^{2+m}} \int_\sigma^\infty d\sigma' \mathcal{H}(\sigma') \\ \times \left( 1 + m + 4 \frac{1 + \rho J(\sigma)}{1 + \rho [J(\sigma) - J(\sigma')]} \right). \end{aligned} \quad (90)$$

It vanishes for  $m = 0$ , as it must because summing the probability over all final states (and without taking the expectation value of anything) just gives 1, but that is already given by the zeroth order in  $\chi_0$ , so all higher orders, and in particular the first order, must vanish. For  $m \gg 1$  we find the same scaling with respect to  $m$  as in the LCF case (35) for  $k = 1$ . We leave a Mellin resummation/transform of the general regime considered in this section for future studies. Using (90) to calculate the standard deviation

$$S^2 \approx \chi_0 \left[ \mathbf{e}_0 \cdot \mathbf{w}_{2,1} \cdot \mathbf{e}_0 - \frac{2}{1 + \rho J} \mathbf{e}_0 \cdot \mathbf{w}_{1,1} \cdot \mathbf{e}_0 \right] \quad (91)$$

gives

$$S^2 = \frac{3b_0\rho}{2[1 + \rho I(\infty)]^4} \int d\sigma \mathcal{H}. \quad (92)$$

Both the classical limit (82) and the LCF limit (21) are local, in the sense that all the integrals over  $\theta = \phi_2 - \phi_1$  have been reduced to the leading-order terms in  $|\theta| \ll 1$  expansions. In contrast, Eq. (92) contains  $\mathcal{H}$ , which is nonlocal, as can be seen from the fact that the  $\theta$  integral in (85) receives in general contributions from  $\theta = \mathcal{O}(1)$ .  $\alpha$  only appears in (92) via  $\rho$ . In particular, the nonlocal term  $\mathcal{H}$  does not depend on  $\alpha$ . In fact, by writing (92) as

$$S^2 = S_{\text{LCF}}^2 \frac{\int d\sigma \mathcal{H}}{\int d\sigma \mathcal{H}_{\text{LCF}}}, \quad (93)$$

where  $S_{\text{LCF}}^2$  is given by (21) and  $\mathcal{H}_{\text{LCF}}$  is the  $a_0 \gg 1$  limit of (85), we see that the dependence on  $\alpha$  is exactly the same as in the LCF limit. In other words, all orders in  $\alpha$  are proportional to the same nonlocal function. For  $a_0 \gg 1$  we recover (21) as we will now show.

### A. LCF

To check the above results we first consider the LCF regime,  $a_0 \gg 1$ . Here we can rescale  $\theta = \hat{\theta}/a_0$  and then expand the integrands in (85) and (86) with  $\hat{\theta}$  as independent of  $a_0$ . This makes the nonlocal terms local. We find

$$\mathcal{H} \approx -\frac{4a_0 F^3}{\pi} \int_{-\infty}^{\infty} d\theta \frac{2 + \theta^2}{\theta^4 \left(1 + \frac{\theta^2}{12}\right)^3} = \frac{55a_0 F^3}{24\sqrt{3}}, \quad (94)$$

where the integration contour goes above the pole at  $\theta = 0$  but below  $\theta = i\sqrt{12}$ , and similarly

$$\mathcal{B} \approx \frac{5\sqrt{3}}{8} a_0 F^3. \quad (95)$$

Restricting for simplicity to linear polarization and spin parallel (or antiparallel) to the magnetic field, we find

$$\mathbf{n}_0 = F^3 \begin{pmatrix} 0 & \frac{3}{2}\epsilon \\ 0 & -\frac{15\sqrt{3}}{16} \end{pmatrix}, \quad \mathbf{n}_1 = F^3 \begin{pmatrix} \frac{55\sqrt{3}}{16} & -\frac{3}{2}\epsilon \\ -\frac{3}{2}\epsilon & \frac{55\sqrt{3}}{16} \end{pmatrix}, \quad (96)$$

and

$$\mathbf{n}_2 = \frac{55}{16\sqrt{3}} F^3 \begin{pmatrix} 1 & 0 \\ 0 & 1 \end{pmatrix}, \quad (97)$$

with the same notation as in Sec. II. By plugging these results into (84) we recover (33), which we obtained there by working with a LCF approximation right from the start.

### B. Perturbative limit

Next we consider the opposite limit, i.e.  $a_0 \ll 1$ . This is a limit that one cannot study using the LCF approximation, since LCF assumes  $a_0 \gg 1$ . Although our approach does not rely on  $a_0$  being large, the smaller  $a_0$  is the longer the pulse would have to be for the incoherent-product approximation to still be valid. So the  $a_0 \ll 1$  limit is perhaps less relevant from an experimental point of view, but it does help to gain some further insights into the behavior of the nonlocal integrals. For  $a_0 \ll 1$  we expand  $\mathcal{H}$  and  $\mathcal{B}$  to  $\mathcal{O}(a_0^2)$ . A  $\mathcal{O}(1/a_0^2)$  term in  $\mathcal{H}$  vanishes upon integrating over  $\theta$ . We Fourier transform the field,

$$\mathbf{f}(\phi) = \int \frac{dw}{2\pi} \mathbf{f}(w) e^{-iw\phi}, \quad (98)$$

where  $\mathbf{f}(\phi) = \mathbf{a}(\phi)/a_0$ . All terms are quadratic in the field, so we have two Fourier variables,  $w_1$  and  $w_2$ , but the  $\sigma$  integral gives a delta function  $\delta(w_1 + w_2)$ . The  $\theta$  integral can, after partial integration, be performed using

$$\int \frac{d\theta}{\theta} \sin(w\theta) = \pi \text{sign}(w). \quad (99)$$

We find

$$\int d\sigma \{\mathcal{H}, \mathcal{B}\} = \left\{ \frac{28}{15}, \frac{4}{3} \right\} \int_0^\infty \frac{dw}{2\pi} w^3 \mathbf{f}(w) \cdot \mathbf{f}(-w). \quad (100)$$

If we expand (90) to  $\mathcal{O}(\alpha)$ , set  $m = 1$ , and use (100), then we find agreement with what one finds by expanding the perturbative, but fully quantum result in Eq. (3.21) in [54] to  $\mathcal{O}(\hbar)$ .

If the field components are proportional to  $\sin(\phi)$  or  $\cos(\phi)$  times a slowly varying envelope, then  $\mathbf{f}(w)$  is sharply peaked at  $w = \pm 1$  and we can approximate  $w^3 \rightarrow 1$  and transform back from  $w$  to  $\sigma$

$$\int d\sigma \{\mathcal{H}, \mathcal{B}\} = \int d\sigma \left\{ \frac{14}{15}, \frac{2}{3} \right\} \frac{\mathbf{a}^2(\sigma)}{a_0^2}. \quad (101)$$

Is this local? Going back to (99), we see that the  $\theta$  integrand is not sharply peaked at  $\theta = 0$ , which one would expect for a local term. Indeed, if we introduce a cutoff  $x$  as

$$\int_{-x}^x \frac{d\theta}{\theta} \sin(\theta) \approx \pi - \frac{2}{x} \cos x, \quad (102)$$

we find a function which converges slowly as  $x \rightarrow \infty$ , which one would interpret as something highly nonlocal. On the other hand, if we instead write (99) as

$$\lim_{\epsilon \rightarrow 0} \int d\theta \frac{\sin(w\theta)}{\theta + i\epsilon}, \quad (103)$$

then we can perform the integral using Cauchy's residue theorem, but the only residue is at  $\theta = -i\epsilon$ , which goes to zero in the limit, suggesting that one instead interpret this as a local term. However, at the end of the day, what we are really interested in is descriptions which help us to find approximations, and if we had made a local expansion right from the start, then we would have obtained the LCF results in (94) and (95), which are very different from the perturbative results (101).

### C. LMF circular polarization

Next we consider the LMF regime for a circularly polarized field,

$$\mathbf{a}(\phi) = a_0 h \left( \frac{\phi}{T} \right) (\sin(\phi) \mathbf{e}_1 + \cos(\phi) \mathbf{e}_2), \quad (104)$$

where  $h$  is an envelope function, e.g.  $h(x) = e^{-x^2}$ , and  $T \gg 1$ . We do not assume that  $a_0$  is large. By rescaling  $\sigma = Tu$  we can expand the integrand to leading order in  $1/T \ll 1$  with  $u$  and  $\theta$  as independent of  $T$  [25]. For example, this gives

$$J(u) = T \int_u^\infty dv h^2(v). \quad (105)$$

When convenient we denote  $a(u) = a_0 h(u)$ . We consider here for simplicity spin parallel to  $\hat{\mathbf{k}}$ , because spin components in the  $\mathbf{e}_1$ - $\mathbf{e}_2$  plane rotate.

We begin with the off-diagonal, local terms. For circularly polarized fields, these off-diagonal terms couple the  $\mathbf{e}_0$  and  $\hat{\mathbf{k}}$  components of the Stokes vector; i.e. these are the components of the Mueller matrix which describe the transition between the unpolarized and longitudinally polarized spin states. The ones from  $\mathbf{n}_0$  in (89) average out. From (88) we find to leading order in  $T \gg 1$ ,

$$\mathbf{n}_1 = \frac{h^2(u)}{a_0} \{ \mathbf{e}_0, \hat{\mathbf{k}} \} + \text{diagonal terms}. \quad (106)$$

Inserting this into (84) gives the off-diagonal terms

$$\begin{aligned} \mathbf{w}_1|_{\text{off}} &= \frac{m \{ \mathbf{e}_0, \hat{\mathbf{k}} \}}{(\rho y)^{m+1} a_0} \int_u^\infty dv \frac{d}{dv} \ln[y - J(v)] \\ &= \frac{m \ln[1 + \rho J(u)]}{a_0 [1 + \rho J(u)]^{1+m}} \{ \mathbf{e}_0, \hat{\mathbf{k}} \}. \end{aligned} \quad (107)$$

From

$$\hat{\mathbf{k}} \cdot \mathbf{w}_1 \cdot \mathbf{e}_0 = \mathbf{e}_0 \cdot \mathbf{w}_1 \cdot \hat{\mathbf{k}} = \hat{\mathbf{k}} \cdot (107) \cdot \mathbf{e}_0 \quad (108)$$

we obtain, to leading order, the difference in the moments when comparing the two cases where the initial state is either spin up or down along the laser propagation

direction, while the final state is unpolarized; or the two cases where the initial state is unpolarized and the final state is either spin up or down. For a constant envelope and  $m = 1$  we recover Eq. (39) in [27]. To compare with an experiment we would only need (107) evaluated at  $u = -\infty$ , but the above expression for finite  $u$  can be used to compare with a numerical solution of (2), and it helps to be able to check the intermediate result already for the first integration steps in  $u$  so that one does not have to wait until the end to check the precision. Equation (107) vanishes for  $m = 0$ , so we will treat this case separately in the next subsection by going to one order higher in  $b_0$ .

Now we turn to the diagonal, nonlocal terms. Expanding to leading order in  $1/T$  gives

$$\Delta a^2 = 4a^2(u) \sin^2 \frac{\theta}{2} \quad (109)$$

and

$$M^2 = 1 + a^2(u) \left( 1 - \text{sinc}^2 \frac{\theta}{2} \right). \quad (110)$$

To facilitate comparison with the monochromatic ( $h$  constant) results in [27], we write

$$\mathcal{H} = \mathcal{I}_1 - \mathcal{I}_0, \quad \mathcal{B} = \frac{1}{2} \mathcal{I}_1, \quad (111)$$

where

$$\mathcal{I}_0 = \frac{1}{a_0^2} \int_0^\infty d\gamma \gamma^2 \mathcal{J}_0 = \frac{8}{\pi a_0^2} \int \frac{d\theta}{\theta \Theta^3} \quad (112)$$

and

$$\mathcal{I}_1 = \frac{1}{a_0^2} \int_0^\infty d\gamma \gamma^2 \mathcal{J}_1 = -\frac{16h^2}{\pi} \int \frac{d\theta}{\theta \Theta^3} \sin^2 \frac{\theta}{2}. \quad (113)$$

We have presented the expressions with  $\mathcal{J}_n$  to compare with [27], but here we will only work with the  $\theta$  integrals.  $\mathcal{I}_0$  and  $\mathcal{I}_1$  have a nontrivial dependence on  $a_0$ .

For  $a_0 \gg 1$  we rescale  $\theta \rightarrow \theta/a_0$ , expand the integrand and find

$$\mathcal{I}_0 \approx \frac{35}{24\sqrt{3}} a_0 h^3(u), \quad \mathcal{I}_1 \approx \frac{5\sqrt{3}}{4} a_0 h^3(u). \quad (114)$$

Equation (114) agrees with (94) and (95). For  $a_0 \ll 1$  we can expand the integrand without rescaling  $\theta$  and then perform partial integration until we have  $\int \sin(\theta)/\theta = \pi$ , which gives

$$\mathcal{I}_0 \approx \frac{2}{5} h^2(u), \quad \mathcal{I}_1 \approx \frac{4}{3} h^2(u). \quad (115)$$

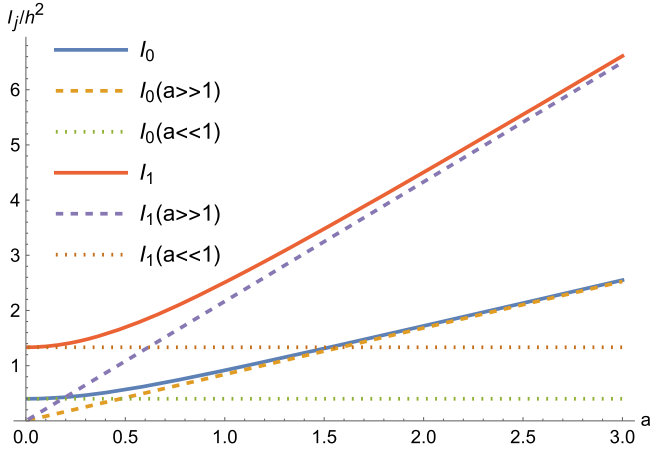


FIG. 7. Solid lines have been obtained by numerically integrating (112) and (113) (along a line parallel to the real axis above the pole at  $\theta = 0$  but below the additional poles due to  $\Theta$ ), dashed lines show (114), and dotted lines show (115).

Equation (115) agrees with (101). These  $a_0 \gg 1$  and  $a_0 \ll 1$  approximations are compared with the exact result in Fig. 7. We see that the full result converges quite quickly to the LCF approximation as  $a = a_0 h(u)$  increases, but the LCF completely breaks down as  $a$  decreases below  $\sim 0.5$ .

For unpolarized initial and final spin states, we find from (90)

$$\mathbf{e}_0 \cdot \mathbf{w}_1 \cdot \mathbf{e}_0 = \frac{3m\rho}{4a_0[1 + \rho J(u)]^{2+m}} \mathcal{T} \int_u^\infty dv (\mathcal{I}_1 - \mathcal{I}_0)(v) \times \left( 1 + m + 4 \frac{1 + \rho J(u)}{1 + \rho[J(u) - J(v)]} \right), \quad (116)$$

and from the  $\mathbf{e}_3 \mathbf{e}_3$  term in (89) we find

$$\hat{\mathbf{k}} \cdot \mathbf{w}_1 \cdot \hat{\mathbf{k}} = \mathbf{e}_0 \cdot \mathbf{w}_1 \cdot \mathbf{e}_0 - \frac{3\rho}{2a_0[1 + \rho J(u)]^m} \mathcal{T} \times \int_u^\infty dv \frac{\mathcal{I}_0(v)}{(1 + \rho[J(u) - J(v)])^2}. \quad (117)$$

For  $m = 0$  and  $u \rightarrow -\infty$  this reduces to

$$\hat{\mathbf{k}} \cdot \chi_0 \mathbf{w}_1 \cdot \hat{\mathbf{k}} = -\frac{3}{2} b_0 \rho \mathcal{T} \int dv \frac{\mathcal{I}_0}{[1 + \rho I(v)]^2}, \quad (118)$$

where

$$I(u) = \mathcal{T} \int_{-\infty}^u dv h^2(v). \quad (119)$$

For a constant envelope we recover Eq. (47) in [27]. Figure 8 shows that the above low-energy approximations agree well with a full numerical solution of (7) for a Sauter-pulse envelope,  $h(u) = \text{sech}^2(u)$ .

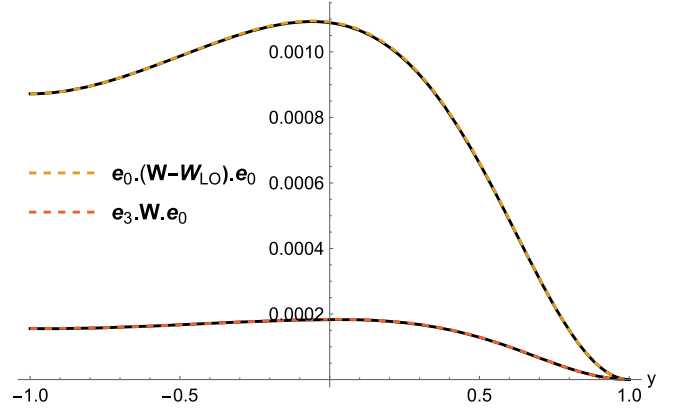


FIG. 8. Comparison of the numerical solution of (7) and the low-energy approximations in (107) and (116), for  $m = 1$  and a circularly polarized field with a Sauter pulse envelope, with  $a_0 = 1$ ,  $b_0 = 10^{-3}$ , and  $\rho\mathcal{T} = 1$ .

For  $m = 0$  we see from (107), (116), and (118) that the Mueller matrix has to first order the following form:

$$\tilde{\mathbf{M}}_0 + \tilde{\mathbf{M}}_1 = \begin{pmatrix} 1 & 0 \\ 0 & 1 - \delta \end{pmatrix}, \quad (120)$$

where  $\delta \propto -$ (118) and  $\delta > 0$ . If the initial state has  $\mathbf{N}_0 = \{1, p\}$  with  $0 \leq |p| \leq 1$  giving the degree of polarization ( $p = 0$  is unpolarized and  $|p| = 1$  is completely polarized), then  $\mathbf{N}_0 \cdot \tilde{\mathbf{M}} \approx \{1, p(1 - \delta)\}$ , so the final state is less polarized, and the degree to which the polarization has been reduced is given by (118).

For  $a_0 \sim 1$  we have  $\rho \ll 1$ , but, as we can see explicitly in the above expressions, the relevant parameter in this regime is  $\rho\mathcal{T}$ , which can be  $\mathcal{O}(1)$  for a sufficiently long pulse,  $\mathcal{T} \gg 1$ , which means we still need to resum the  $\alpha$  expansion.

The standard deviation is obtained directly from (92). Using (114), we find for  $a_0 \gg 1$

$$S^2 = \frac{55\chi_0\rho}{16\sqrt{3}[1 + \rho I(\infty)]^4} \mathcal{T} \int du h^3(u), \quad (121)$$

which agrees with what one finds by taking the LCF limit first, i.e. (21). For  $a_0 \ll 1$  we find, using (115),

$$S^2 = \frac{7b_0\rho}{5[1 + \rho I(\infty)]^4} \mathcal{T} \int du h^2(u). \quad (122)$$

#### D. LMF—Off-diagonal element for $m = 0$

The zeroth moment is special because the zeroth order in  $\chi_0$  is just the identity matrix,

$$\tilde{\mathbf{M}} = \mathbf{1} + \Delta\mathbf{M}. \quad (123)$$

Because of unitarity we also have  $\Delta \mathbf{M} \cdot \{1, \mathbf{0}\} = \mathbf{0}$ , since if we sum the zeroth moment over the final spin, then we have summed the probability over all possible final states. Thus, if we restrict to spin parallel to the laser wave vector  $\hat{\mathbf{k}}$ , then a general Mueller matrix would be  $2 \times 2$ , but, for the zeroth moment, two of the four elements are trivial:

$$\Delta \mathbf{M} = \begin{pmatrix} 0 & B \\ 0 & A \end{pmatrix}. \quad (124)$$

$A$  is given by (118) and is  $\mathcal{O}(b_0)$ . Equation (107) shows that  $B$  vanishes at  $\mathcal{O}(b_0)$ . We will now show that  $B = \mathcal{O}(b_0^2)$ .

From (2) we have

$$\begin{aligned} \partial_\sigma B = & - \int_0^1 dq [\mathbf{e}_0 \cdot \mathbf{M}_L \cdot \mathbf{e}_0 B(b_0) \\ & + \mathbf{e}_0 \cdot \mathbf{M}_C \cdot \mathbf{e}_0 B([1 - q]b_0)] \\ & - \int_0^1 dq [\mathbf{e}_0 \cdot \mathbf{M}_L \cdot \mathbf{e}_3 A(b_0) \\ & + \mathbf{e}_0 \cdot \mathbf{M}_C \cdot \mathbf{e}_3 A([1 - q]b_0)]. \end{aligned} \quad (125)$$

Since  $\mathbf{e}_0 \cdot \mathbf{M}_L \cdot \mathbf{e}_0 = -\mathbf{e}_0 \cdot \mathbf{M}_C \cdot \mathbf{e}_0$  and  $\mathbf{e}_0 \cdot \mathbf{M}_L \cdot \mathbf{e}_3 = -\mathbf{e}_0 \cdot \mathbf{M}_C \cdot \mathbf{e}_3$ , we have to leading order

$$\partial_\sigma B = f_1 b_0 \partial_{b_0} B + f_2 b_0 \partial_{b_0} A, \quad (126)$$

where, from (81) and (106),

$$\begin{aligned} f_1 = & \int dq q \mathbf{e}_0 \cdot \mathbf{M}_C \cdot \mathbf{e}_0 \approx \frac{2}{3} ab_0 a^2(\sigma) \approx \frac{2}{3} ab_0 a^2(u), \\ f_2 = & \int dq q \mathbf{e}_0 \cdot \mathbf{M}_C \cdot \mathbf{e}_3 \approx -\frac{2}{3} ab_0^2 a^2(u). \end{aligned} \quad (127)$$

Using the method of characteristics as above, we find

$$B = -3b_0^2 \rho T \int_u^\infty dv \mathcal{I}_0(v) \frac{\ln(1 + \rho[J(u) - J(v)])}{(1 + \rho[J(u) - J(v)])^3}. \quad (128)$$

For a constant envelope  $h = 1$ , we recover<sup>5</sup> Eq. (48) in [27]. If the initial state is unpolarized, then  $B(u \rightarrow -\infty)$  gives the degree of longitudinal polarization in the final state. It is small due to the factor of  $b_0^2$ , but it shows that for circular polarization there is a nonzero induced (longitudinal) polarization, in contrast to linear polarization where the induced polarization averages out due to the oscillations of the field.

### E. LMF linear polarization

In this section we consider fields with linear polarization which oscillate in a symmetric way, so that some spin effects average out. The spin components in the  $\hat{\mathbf{E}}\text{-}\hat{\mathbf{k}}$  plane

<sup>5</sup> $\mathcal{T}$  in [27] is equal to  $\alpha \mathcal{T}$  in the notation here.

rotates. There is no induced polarization (Sokolov-Ternov effect) in this case since the components, which would otherwise lead to such effects in the  $\hat{\mathbf{B}}$  direction, oscillate and average out. However, this does not mean that there cannot be any nontrivial change in the spin along  $\hat{\mathbf{B}}$ . If the initial state is polarized, then there can be depolarization, since the diagonal element  $\hat{\mathbf{B}}_0 \cdot \tilde{\mathbf{M}} \cdot \hat{\mathbf{B}}_0$  is different from  $\mathbf{e}_0 \cdot \tilde{\mathbf{M}} \cdot \mathbf{e}_0$ . From the  $\mathbf{e}_2 \mathbf{e}_2$  term in (89) we find

$$\begin{aligned} \hat{\mathbf{B}}_0 \cdot \mathbf{w}_1 \cdot \hat{\mathbf{B}}_0 = & \mathbf{e}_0 \cdot \mathbf{w}_1 \cdot \mathbf{e}_0 - \frac{3\rho}{2a_0[1 + \rho J(\sigma)]^m} \\ & \times \int_\sigma^\infty d\sigma' \frac{\mathcal{B}(\sigma')}{(1 + \rho[J(\sigma) - J(\sigma')])^2}, \end{aligned} \quad (129)$$

where  $\mathbf{e}_0 \cdot \mathbf{w}_1 \cdot \mathbf{e}_0$  is given by (90). It is not obvious at this point, but we will show below that  $\mathcal{B} > 0$ , so for  $m = 0$ , the  $\mathbf{e}_0$  and  $\hat{\mathbf{B}}_0$  components of the Mueller matrix are given by

$$\tilde{\mathbf{M}}_0 + \tilde{\mathbf{M}}_1 = \begin{pmatrix} 1 & 0 \\ 0 & 1 - \delta \end{pmatrix}, \quad (130)$$

where  $\delta > 0$ . This implies depolarization similar to (120), except that (120) is for the  $\mathbf{e}_0 - \hat{\mathbf{k}}$  components, while (130) is for the  $\mathbf{e}_0 - \hat{\mathbf{B}}_0$  components.

Now we consider a field on the form

$$\mathbf{a}(\phi) = a_0 h \left( \frac{\phi}{T} \right) \sin(\phi + \Delta) \mathbf{e}_1, \quad (131)$$

where  $\Delta$  is a constant and  $h$  is an envelope similar to the circular case (104). We can again find the leading order in  $1/T \ll 1$  by rescaling  $\sigma = Tu$  and consider  $u$  and  $\theta$  as independent of  $T$ . We have

$$J(u) \approx T \int_u^\infty dv [h(v) \cos(Tv + \Delta)]^2 \approx \frac{T}{2} \int_u^\infty dv h^2(v). \quad (132)$$

For the effective mass one finds

$$\begin{aligned} M^2 = & 1 + \frac{a^2(u)}{2} \left( 1 - \text{sinc}(\theta) + 2\sin^2(Tu + \Delta) \right. \\ & \left. \times \left[ \text{sinc}(\theta) - \text{sinc}^2\left(\frac{\theta}{2}\right) \right] \right). \end{aligned} \quad (133)$$

$M^2$  only depends on  $u$  via the envelope  $a(u)$  in the circular case (110), but (133) also has a rapidly oscillating term. If the  $\sigma$  integrand had been linear in  $M^2$  we could have replaced  $\sin^2(Tu + \Delta) \rightarrow 1/2$ , and then (133) would have reduced to the circular case (110) but with  $a_0 \rightarrow a_0/\sqrt{2}$ . However, the integrands in (85) and (86) are not linear in  $M^2$ . Instead we have integrands of the form

$$F[a(u), \sin^2(\mathcal{T}u + \Delta)], \quad (134)$$

where  $F$  is a nonlinear function. We introduce a temporary variable  $\delta$  and then Taylor expand

$$F[a, \delta \sin^2(\mathcal{T}u + \Delta)] = \sum_{n=0}^{\infty} F_n[a] \delta^n \sin^{2n}(\mathcal{T}u + \Delta). \quad (135)$$

Next we write

$$\begin{aligned} \sin^{2n}(\varphi) &= \left( \frac{e^{i\varphi} - e^{-i\varphi}}{2i} \right)^{2n} \\ &= \frac{(2n)!}{4^n (n!)^2} + \text{oscillating terms}. \end{aligned} \quad (136)$$

We can neglect the oscillating terms since they oscillate rapidly for  $\mathcal{T} \gg 1$ . The sum

$$\sum_{n=0}^{\infty} F_n[a] \delta^n \frac{(2n)!}{4^n (n!)^2} \quad (137)$$

might look more complicated than (135), but *Mathematica* has no problem summing this series in the cases we have considered. Applying this to (86) and (85) gives

$$\mathcal{B} = -\frac{h^2(u)}{\pi} \int d\theta \frac{(4X + 3Y) \sin^2\left(\frac{\theta}{2}\right)}{X^{5/2} (X + Y)^{3/2} \theta^4} \quad (138)$$

and

$$\mathcal{H} = 2\mathcal{B} - \frac{1}{\pi a_0^2} \int d\theta \frac{8X^2 + 8XY + 3Y^2}{\theta^4 X^{5/2} (X + Y)^{5/2}}, \quad (139)$$

where

$$\begin{aligned} X &= 1 + \frac{a^2(u)}{2} [1 - \text{sinc}(\theta)], \\ Y &= a^2(u) \left[ \text{sinc}(\theta) - \text{sinc}^2\left(\frac{\theta}{2}\right) \right]. \end{aligned} \quad (140)$$

We can obtain the same results by replacing

$$F[a(u), \sin^2(\mathcal{T}u + \Delta)] \rightarrow \frac{1}{\pi} \int_{-\pi/2}^{\pi/2} d\varphi F[a(u), \sin^2(\varphi)], \quad (141)$$

since the integral selects the terms in (136) which do not oscillate. The approach using (141) can be found in the literature [32]. Note that  $\mathcal{B}/h^2$  and  $\mathcal{H}/h^2$  are only functions of one variable,  $a(u)$ , so one can make numerical interpolation functions of them for  $0 < a < a_0$  without choosing any specific envelope  $h(u)$ , and then afterwards one can

apply the interpolation to e.g.  $h = e^{-u^2}$ ,  $h = \text{sech}^2(u)$ , or any other envelope.

For  $a_0 \gg 1$  we can perform the  $\theta$  integral by rescaling  $\theta \rightarrow \theta/a$  and then expanding the integrand to leading order,

$$\mathcal{B} \approx -\frac{6\sqrt{3}}{\pi} a_0 h^3 \int d\theta \frac{48 + \theta^2}{\theta^2 (12 + \theta^2)^{5/2}} = \frac{5a_0 h^3}{2\sqrt{3}\pi} \quad (142)$$

and similarly

$$\mathcal{H} \approx \frac{55a_0 h^3}{18\sqrt{3}\pi}. \quad (143)$$

Plugging (142) into (129) gives for  $m = 0$

$$\hat{\mathbf{B}}_0 \cdot \chi_0 \mathbf{w}_1 \cdot \hat{\mathbf{B}}_0 = -\frac{5\sqrt{3}\chi_0 \rho \mathcal{T}}{4\pi} \int du \frac{h^3(u)}{[1 + \rho I(u)]^2}, \quad (144)$$

where

$$I(u) = \frac{\mathcal{T}}{2} \int_{-\infty}^u dv h^2(v). \quad (145)$$

Plugging (143) into (92) gives

$$S^2 = \frac{55\chi_0 \rho \mathcal{T}}{12\sqrt{3}\pi [1 + \rho I(\infty)]^4} \int du h^3(u). \quad (146)$$

Equation (144) agrees with the diagonal component of (17), and (146) agrees with (21), but to see that we need to simplify (17) and (21). We have  $F(\sigma) \approx h(u) |\cos(\mathcal{T}u + \Delta)|$ , which makes the integral in (17) and (21) nonanalytic. We can write them as

$$\begin{aligned} &\int d\sigma h^3\left(\frac{\sigma - \Delta}{\mathcal{T}}\right) |\cos^3(\sigma)| G\left(\frac{\sigma - \Delta}{\mathcal{T}}\right) \\ &\approx \sum_{n=-\infty}^{\infty} h^3\left(\frac{n\pi}{\mathcal{T}}\right) G\left(\frac{n\pi}{\mathcal{T}}\right) \int_{-\pi/2}^{\pi/2} d\sigma \cos^3(\sigma) \\ &\approx \frac{4\mathcal{T}}{3\pi} \int du h^3(u) G(u), \end{aligned} \quad (147)$$

where  $G$  just stands for the rest of the integrand. Thus, we should multiply (94) and (95) by  $4/(3\pi)$  and replace  $F \rightarrow h$ , and then we find agreement with (143) and (142). And by using (147) on (17) and (21) we recover (144) and (146).

For  $a_0 \ll 1$  we can expand the integrands in (138) and (139) without rescaling  $\theta$ . We find

$$\mathcal{B} = \frac{h^2}{3}, \quad \mathcal{H} = \frac{7h^2}{15}. \quad (148)$$

Equation (148) agrees with (101). The perturbative (148) and LCF approximations (142) and (143) are compared with the exact result in Fig. 9. The conclusion from Fig. 9 is

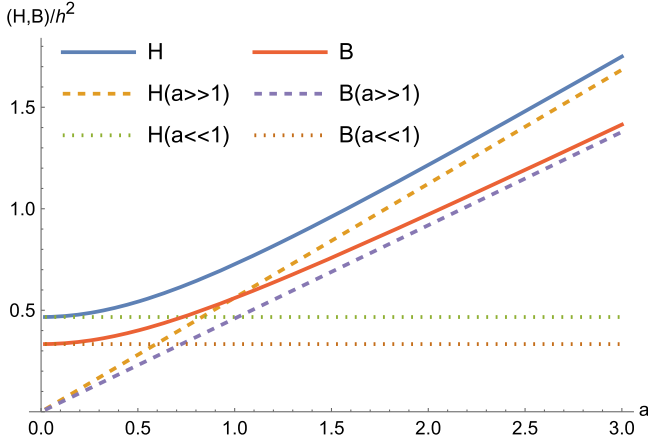


FIG. 9.  $\mathcal{B}$  and  $\mathcal{H}$  divided by  $h^2$ . Solid lines are obtained by numerically integrating (138) and (139), dashed lines show (142) and (143), and dotted lines show (148).

similar to the circular case in Fig. 7; i.e. the LCF approximation converges to the exact result as  $a$  increases, though more slowly in this case, and breaks down as  $a$  decreases.

### F. Bichromatic field

For a field which is linearly polarized and almost monochromatic, as in (131), the off-diagonal terms in (88) and (89) tend to average out due to the oscillations, which means there is no (or a negligible) induced polarization. However, this is not necessarily the case if we instead consider an almost bichromatic field

$$\mathbf{a}(\phi) = a_0 h \left( \frac{\phi}{\mathcal{T}} \right) [a_1 \sin(\phi) + a_2 \sin(2\phi + \Delta)] \mathbf{e}_1. \quad (149)$$

Such fields were studied in [15,16], for the same reason. Instead of (132) we have

$$J \approx (a_1^2 + 4a_2^2) \frac{\mathcal{T}}{2} \int_u^\infty dv h^2(v). \quad (150)$$

The off-diagonal terms in (88) and (89) are proportional to

$$\begin{aligned} \frac{a^3(\sigma)}{(a_0 h)^3} &\approx a_1^3 \cos^3(\sigma) + 6a_1^2 a_2 \cos^2(\sigma) \cos(2\sigma + \Delta) \\ &+ 12a_1 a_2^2 \cos(\sigma) \cos^2(2\sigma + \Delta) + 8a_2^3 \cos^3(2\sigma + \Delta). \end{aligned} \quad (151)$$

After writing  $\cos$  in terms of  $e^{i\sigma}$ , one finds that only the second term contains a nonoscillating part,

$$(151) \approx \frac{3}{2} a_1^2 a_2 \cos \Delta + \text{oscillating terms}. \quad (152)$$

So, from (88) and (89) we find

$$\mathbf{n}_1 \approx \frac{9}{4} a_1^2 a_2 \cos(\Delta) h^3 \{ \mathbf{e}_0, \mathbf{e}_2 \} + \text{diagonal terms} \quad (153)$$

and

$$\mathbf{n}_0 \approx -\frac{9}{4} a_1^2 a_2 \cos(\Delta) h^3 \mathbf{e}_0 \mathbf{e}_2 + \text{diagonal terms}. \quad (154)$$

Since these off-diagonal terms are already local, they agree<sup>6</sup> with what one finds from the off-diagonal terms of the LCF approximation in (96) even without making any expansion in  $1/a_0$ . For  $m = 0$  we find

$$\mathbf{e}_0 \cdot \mathbf{w}_1 \cdot \mathbf{e}_2 = -\frac{9}{4} a_1^2 a_2 \rho \cos \Delta \int du \frac{h^3(u)}{[1 + \rho I(u)]^2}, \quad (155)$$

where

$$I(u) = (a_1^2 + 4a_2^2) \frac{\mathcal{T}}{2} \int_{-\infty}^u dv h^2(v). \quad (156)$$

Equation (155) gives the polarization of the final state if the initial state is unpolarized. It vanishes if either  $a_1 = 0$  or  $a_2 = 0$ , i.e. if we have a monochromatic rather than bichromatic field, as expected.

## VI. SPIN PERPENDICULAR TO MAGNETIC FIELD

In this section we consider the components of the Stokes vector which describe spin perpendicular to the magnetic field. We consider a linearly polarized field, which means the  $\mathbf{e}_0$  and  $\hat{\mathbf{B}}_0$  components, which we studied in Sec. II, decouple from the  $\hat{\mathbf{E}}_0$  and  $\hat{\mathbf{k}}$  components, which we will now study. Here  $\hat{\mathbf{E}}_0$  is the constant axis parallel to the electric field,  $\hat{\mathbf{k}}$  is the axis of propagation, and  $\hat{\mathbf{B}}_0 = \hat{\mathbf{E}}_0 \times \hat{\mathbf{k}}$ . The off-diagonal elements of  $\mathbf{M}_L$  in the  $\hat{\mathbf{E}}_0 - \hat{\mathbf{k}}$  space [see (A16)] act as a rotation matrix,

$$\mathbf{R}(\sigma, b_0) = \frac{\alpha}{b_0} (\hat{\mathbf{k}} \hat{\mathbf{E}} - \hat{\mathbf{E}} \hat{\mathbf{k}}) \int_0^1 dq q \frac{\text{Gi}(\xi)}{\sqrt{\xi}}, \quad (157)$$

where  $\xi = (r/\chi(\sigma))^{2/3}$ ,  $r = (1/s) - 1$ ,  $s = 1 - q$ , and Gi is the Scorer function.<sup>7</sup> For linear polarization we have

$$\hat{\mathbf{k}} \hat{\mathbf{E}} - \hat{\mathbf{E}} \hat{\mathbf{k}} = \epsilon(\sigma) (\hat{\mathbf{k}} \hat{\mathbf{E}}_0 - \hat{\mathbf{E}}_0 \hat{\mathbf{k}}), \quad (158)$$

so  $\mathbf{R}$  is proportional to a constant matrix. So, if we write

$$\mathbf{M} = \exp \left\{ \int_\sigma^\infty d\sigma' \mathbf{R}(\sigma') \right\} \mathbf{M}', \quad (159)$$

<sup>6</sup>Note  $\mathbf{e}_2 = -\hat{\mathbf{B}}_0$  as explained in [25].

<sup>7</sup>Gi also appears in the results in [55] for the loop, though not as the cross term between the loop and the zeroth order and hence not as a Mueller matrix.

then

$$\frac{\partial \mathbf{M}}{\partial \sigma} + \mathbf{R} \cdot \mathbf{M} = \exp \left\{ \int_{\sigma}^{\infty} d\sigma' \mathbf{R}(\sigma') \right\} \frac{\partial \mathbf{M}'}{\partial \sigma}, \quad (160)$$

which, at first sight, might suggest that by multiplying (2) with  $e^{-\int \dots}$  one would obtain an equation for  $\mathbf{M}'$  which does not involve  $\mathbf{R}$ . However, that is not the case, because in the term with  $\mathbf{M}_C$  we would have

$$\begin{aligned} & \exp \left\{ - \int_{\sigma}^{\infty} d\sigma' \mathbf{R}(\sigma', b_0) \right\} \cdot \mathbf{M}_C \\ & \cdot \exp \left\{ - \int_{\sigma}^{\infty} d\sigma' \mathbf{R}(\sigma', [1-q]b_0) \right\} \neq \mathbf{M}_C. \end{aligned} \quad (161)$$

To resolve this issue we consider the  $\chi \ll 1$  expansion of

$$\mathcal{G}(\chi) := \int_0^1 dq q \frac{\text{Gi}(\xi)}{\sqrt{\xi}}. \quad (162)$$

To find a  $\chi$  expansion we calculate the Mellin transform<sup>8</sup>

$$\mathcal{G}(S) = \int_0^{\infty} d\chi \chi^{S-1} \mathcal{G}(\chi). \quad (163)$$

We change variable from  $q$  to  $\xi$ , so that  $\chi$  does not appear in  $\text{Gi}$ , and then we perform the  $\chi$  integral first. We find

$$\mathcal{G}(S) = \int_0^{\infty} d\xi \frac{3\pi S(1+S)}{4 \sin(\pi S)} \xi^{-\frac{3}{2}(1+S)} \text{Gi}(\xi) \quad (164)$$

provided  $-2 < \text{Re}S < 1$ . Next we express the Scorer function as an integral,

$$\text{Gi}(\xi) = \int_0^{\infty} \frac{d\tau}{\pi} \sin \left( \frac{\tau^3}{3} + \xi\tau \right). \quad (165)$$

Then we perform first the  $\xi$  integral and then the  $\tau$  integral. For

$$-1 < \text{Re}S < -\frac{1}{3} \quad (166)$$

we find

$$\mathcal{G}(S) = \frac{\pi}{4} 3^{(1+S)/2} S \frac{\Gamma \left[ -\frac{1+3S}{2} \right]}{\Gamma \left[ -\frac{1+S}{2} \right] \cos^2 \left[ \frac{\pi}{2} S \right]}. \quad (167)$$

The inverse Mellin transform is given by

<sup>8</sup>Mellin transforms have also been used in e.g. [56,57].

$$\mathcal{G}(\chi) = \int \frac{dS}{2\pi i} \chi^{-S} \mathcal{G}(S), \quad (168)$$

where the integration contour crosses the real axis at some point in the range (166). If we close the contour around the real axis with  $S > -1/3$ , we obtain a  $\chi \gg 1$  expansion. Here we are instead interested in the  $\chi \ll 1$  expansion, which we obtain by closing the contour around the real axis with  $S < -1$ . We have a simple pole at  $S = -1$ , which gives the leading order, and double poles at  $S = -3, -5, -7, \dots$ , which give higher orders. We find [25]

$$\mathcal{G}(\chi) = \mathcal{G}_{\text{LO}}(\chi) + \mathcal{O}(\chi^3 \ln(\chi)), \quad (169)$$

where the leading order is (cf. e.g. [42])

$$\mathcal{G}_{\text{LO}}(\chi) = \frac{\chi}{2\pi}. \quad (170)$$

The higher orders are given by

$$\begin{aligned} \Delta \mathcal{G}(\chi) &= \sum_{n=1}^{\infty} \frac{\sqrt{3}}{2\pi} \left( \frac{\chi}{\sqrt{3}} \right)^{2n+1} \frac{\Gamma[1+3n]}{\Gamma[n]} (1+2n) \\ &\times \left( 2 \ln \left( \frac{\chi}{\sqrt{3}} \right) - 2\gamma_E + \frac{2}{1+2n} + 3H_{3n} - H_{n-1} \right), \end{aligned} \quad (171)$$

where  $\Delta \mathcal{G} = \mathcal{G} - \mathcal{G}_{\text{LO}}$ ,  $\gamma_E = 0.577\dots$  is Euler's constant, and  $H_n = \sum_{k=1}^n 1/k$  is the harmonic number. The coefficients  $a_n$  multiplying  $(\chi/\sqrt{3})^{2n+1}$  grow asymptotically as  $a_n/a_{n+1} \sim 1/(27n^2)$ , so this is an asymptotic series. This series has a different mathematical structure compared to the corresponding series for the  $\mathbf{e}_0$  and  $\hat{\mathbf{B}}_0$  components, which e.g. do not have  $\ln(\chi)$  terms.

A convenient and fast way to numerically compute  $\mathcal{G}(\chi)$  exactly is to integrate (168) along a contour  $C_1$  which is parallel to the imaginary axis with e.g.  $\text{Re}(S) = -1/2$ . In our numerical implementation (with *Mathematica*), this is in fact much faster than directly integrating (162). An equally convenient way to compute  $\Delta \mathcal{G}(\chi)$  is to integrate (168) with exactly the same integrand (167) but along a contour  $C_2$  which is parallel to the imaginary axis with  $\text{Re}(S) = -2$ . This works because we can deform  $C_1$  to  $C_2$  plus a small loop around the pole at  $S = -1$ , and the loop integral gives exactly  $\mathcal{G}_{\text{LO}}$ , so omitting this loop gives  $\mathcal{G} - \mathcal{G}_{\text{LO}}$  exactly.

Inserting the leading order into the rotation matrix gives

$$\mathbf{R}_{\text{LO}}(\sigma) = \frac{\alpha\chi}{2\pi b_0} (\hat{\mathbf{k}} \hat{\mathbf{E}} - \hat{\mathbf{E}} \hat{\mathbf{k}}) = \frac{\alpha a_0 F(\sigma)}{2\pi} (\hat{\mathbf{k}} \hat{\mathbf{E}} - \hat{\mathbf{E}} \hat{\mathbf{k}}), \quad (172)$$

where  $F$  is given in (8). There are two important things to note here. First, we can write  $\alpha a_0 = \frac{3\rho}{2\chi_0}$ , so, since we

consider  $\rho = \mathcal{O}(1)$ , the rotation matrix is proportional to a large factor for  $\chi \ll 1$ . This means the spin rotates on a much faster timescale compared to the change in the momentum. That could be problematic for numerical computations if we work with  $\mathbf{M}$ . However, the second thing to note is that, unlike  $\mathbf{R}$ ,  $\mathbf{R}_{\text{LO}}$  does not depend on  $b_0$ . Also,  $\mathbf{R} - \mathbf{R}_{\text{LO}}$  is small for  $\chi \ll 1$ , so the fast oscillations are determined by  $\mathbf{R}_{\text{LO}}$ . We therefore exponentiate  $\mathbf{R}_{\text{LO}}$  rather than  $\mathbf{R}$ , by substituting

$$\mathbf{M} = \exp \left\{ \int_{\sigma}^{\infty} d\sigma' \mathbf{R}_{\text{LO}}(\sigma') \right\} \bar{\mathbf{M}} \quad (173)$$

into (B1). [This works for both the moments  $\bar{\mathbf{M}}(b_0, m)$  and the cumulative distribution function of the spectrum  $\mathbf{M}(b_0, x)$ .] For a linearly polarized field we can write

$$\int_{\sigma}^{\infty} d\sigma' \mathbf{R}_{\text{LO}} = \varphi (\hat{\mathbf{k}} \hat{\mathbf{E}}_0 - \hat{\mathbf{E}}_0 \hat{\mathbf{k}}), \quad (174)$$

where

$$\varphi = \frac{\alpha a_0}{2\pi} \int_{\sigma}^{\infty} d\sigma' \epsilon(\sigma') F(\sigma'). \quad (175)$$

Since  $(\hat{\mathbf{k}} \hat{\mathbf{E}}_0 - \hat{\mathbf{E}}_0 \hat{\mathbf{k}})^2 = -(\hat{\mathbf{E}}_0 \hat{\mathbf{E}}_0 + \hat{\mathbf{k}} \hat{\mathbf{k}})$ , we have

$$\begin{aligned} & \exp \left\{ \int_{\sigma}^{\infty} d\sigma' \mathbf{R}_{\text{LO}}(\sigma') \right\} \\ &= \mathbf{e}_0 \mathbf{e}_0 + \hat{\mathbf{B}}_0 \hat{\mathbf{B}}_0 \\ &+ (\hat{\mathbf{E}}_0 \hat{\mathbf{E}}_0 + \hat{\mathbf{k}} \hat{\mathbf{k}}) \cos \varphi + (\hat{\mathbf{k}} \hat{\mathbf{E}}_0 - \hat{\mathbf{E}}_0 \hat{\mathbf{k}}) \sin \varphi. \end{aligned} \quad (176)$$

We find

$$\begin{aligned} \frac{\partial \bar{\mathbf{M}}}{\partial \sigma} &= -\Delta \mathbf{R} \cdot \bar{\mathbf{M}} - \int_0^1 dq \left\{ \mathbf{M}'_L \cdot \bar{\mathbf{M}}(b_0, x) \right. \\ &+ \left. \theta(x - q) \mathbf{M}'_C \cdot \bar{\mathbf{M}} \left( [1 - q] b_0, \frac{x - q}{1 - q} \right) \right\}, \end{aligned} \quad (177)$$

where  $\mathbf{M}'_L$  is  $\mathbf{M}_L$  in (A16) without the  $\hat{\mathbf{k}} \hat{\mathbf{E}} - \hat{\mathbf{E}} \hat{\mathbf{k}}$  term,

$$\begin{aligned} \mathbf{M}'_C &= \exp \left\{ - \int_{\sigma}^{\infty} d\sigma' \mathbf{R}_{\text{LO}}(\sigma') \right\} \\ &\cdot \mathbf{M}_C \cdot \exp \left\{ \int_{\sigma}^{\infty} d\sigma' \mathbf{R}_{\text{LO}}(\sigma') \right\} \end{aligned} \quad (178)$$

and

$$\Delta \mathbf{R} = \mathbf{R} - \mathbf{R}_{\text{LO}}. \quad (179)$$

Using (176), we see that the  $\mathbf{e}_0$  and  $\hat{\mathbf{B}}_0$  components of  $\mathbf{M}'_C$  are the same as  $\mathbf{M}_C$ .  $\mathbf{M}_C$  also contains terms proportional to

$\hat{\mathbf{E}}_0 \hat{\mathbf{E}}_0$  and  $\hat{\mathbf{k}} \hat{\mathbf{k}}$ . Denoting the proportionality coefficients  $a$  and  $b$ , we have

$$\begin{aligned} & [(\hat{\mathbf{E}}_0 \hat{\mathbf{E}}_0 + \hat{\mathbf{k}} \hat{\mathbf{k}}) \cos \varphi - (\hat{\mathbf{k}} \hat{\mathbf{E}}_0 - \hat{\mathbf{E}}_0 \hat{\mathbf{k}}) \sin \varphi] \cdot [a \hat{\mathbf{E}}_0 \hat{\mathbf{E}}_0 + b \hat{\mathbf{k}} \hat{\mathbf{k}}] \\ & \cdot [(\hat{\mathbf{E}}_0 \hat{\mathbf{E}}_0 + \hat{\mathbf{k}} \hat{\mathbf{k}}) \cos \varphi + (\hat{\mathbf{k}} \hat{\mathbf{E}}_0 - \hat{\mathbf{E}}_0 \hat{\mathbf{k}}) \sin \varphi] \\ &= \frac{a+b}{2} \begin{pmatrix} 1 & 0 \\ 0 & 1 \end{pmatrix} + \frac{b-a}{2} \begin{pmatrix} -\cos(2\varphi) & \sin(2\varphi) \\ \sin(2\varphi) & \cos(2\varphi) \end{pmatrix} \\ &=: \mathbf{M}'_{C,D} + \mathbf{M}'_{C,O}, \end{aligned} \quad (180)$$

where the  $\{1, 0\}$  and  $\{0, 1\}$  elements in this 2D representation correspond, respectively, to  $\hat{\mathbf{E}}_0$  and  $\hat{\mathbf{k}}$ .  $\mathbf{M}'_{C,O}$  in (180) oscillates rapidly, and one might expect that it is therefore negligible. Proving that is perhaps a bit more nontrivial than what one might naively expect. However, we show in Appendix D that one can indeed neglect  $\mathbf{M}'_{C,O}$  for the first couple of orders in  $\chi \ll 1$ . It is not negligible for  $\chi \lesssim 1$ , but then the oscillations are not fast anyway, which removes the motivation for trying to factor out the oscillations in the first place; i.e. then one might just as well work directly with  $\mathbf{W}$  rather than with  $\bar{\mathbf{W}}$ . Thus, we have factored out most of the spin precession. In PIC codes [17] this is instead included by solving the Thomas-Bargmann-Michel-Telegdi equation [58,59].

For  $\rho = \mathcal{O}(1)$  we have  $\varphi = \mathcal{O}(1/\chi)$ , and then even quite small changes in the pulse shape can lead to  $\mathcal{O}(1)$  changes in  $\varphi$ , which, although relatively small compared to  $\varphi = \mathcal{O}(1/\chi)$ , can completely change the values of  $\cos \varphi$  and  $\sin \varphi$ . For an oscillating field, the integral in (175) can be identically zero. However, even a small deviation from such a symmetrically oscillating field could lead to  $\mathcal{O}(1)$  changes to  $\varphi$ . For a Sauter pulse the rotation angle (175) is equal to  $\varphi = 3\rho/(2\pi\chi_0)$ , so  $\varphi \sim 477\rho$  for  $\chi_0 = 10^{-3}$ .

### A. Degree of polarization from Frobenius norm

If the initial Stokes vector is given by

$$\mathbf{N}_0 = \mathbf{e}_0 + p_B \hat{\mathbf{B}}_0 + p_{Ek} \mathbf{n}, \quad (181)$$

where  $p_B$  and  $p_{Ek}$  are degrees of polarization and

$$\mathbf{n}(\mu) = \cos(\mu) \hat{\mathbf{E}}_0 + \sin(\mu) \hat{\mathbf{k}} \quad (182)$$

is a unit vector in the spin-rotation plane, then from (176) we find upon projecting the Mueller matrix as in (1)

$$\mathbf{n}(\mu) \cdot \exp \left\{ \int_{\sigma}^{\infty} d\sigma' \mathbf{R}_{\text{LO}}(\sigma') \right\} = \mathbf{n}(\mu - \varphi). \quad (183)$$

Thus,  $\mathbf{R}_{\text{LO}}$  rotates the initial Stokes vector in the  $\hat{\mathbf{E}} - \hat{\mathbf{k}}$  plane. Each component of  $\mathbf{n}(\mu - \varphi) \cdot \bar{\mathbf{M}}$  will be proportional to  $\cos(\mu - \varphi)$  or  $\sin(\mu - \varphi)$  and will therefore be sensitive to the value of  $\varphi$ . It can therefore be difficult to predict in

which direction in the  $\hat{\mathbf{E}}\text{-}\hat{\mathbf{k}}$  plane the final spin will be, and if one makes an average over experimental runs with slightly different conditions, then these components might average out. However, for the degree of polarization we have

$$\begin{aligned} p_f^2 &:= [\mathbf{n}(\mu - \varphi) \cdot \bar{\mathbf{M}} \cdot \mathbf{n}(\nu)]^2 \\ &\quad + [\mathbf{n}(\mu - \varphi) \cdot \bar{\mathbf{M}} \cdot \mathbf{n}(\nu + \pi/2)]^2 \\ &= [M_{EE}^2 + M_{Ek}^2] \cos^2(\mu - \varphi) + [M_{kE}^2 + M_{kk}^2] \sin^2(\mu - \varphi) \\ &\quad + [M_{EE}M_{kE} + M_{Ek}M_{kk}] \sin[2(\mu - \varphi)], \end{aligned} \quad (184)$$

which averages to

$$\begin{aligned} \langle p_f^2 \rangle &= \frac{1}{2} [M_{EE}^2 + M_{Ek}^2 + M_{kE}^2 + M_{kk}^2] \\ &= \frac{1}{2} \text{tr}(\bar{\mathbf{M}}_{(\perp)}^T \bar{\mathbf{M}}_{(\perp)}) = \frac{1}{2} \|\bar{\mathbf{M}}_{(\perp)}\|_F^2, \end{aligned} \quad (185)$$

where  $\bar{\mathbf{M}}_{(\perp)}$  is the part of  $\bar{\mathbf{M}}$  in the  $\hat{\mathbf{E}}\text{-}\hat{\mathbf{k}}$  plane and  $\|\dots\|_F$  is the Frobenius norm. We emphasize that the above is a mathematical way to extract a quantity that is not sensitive to  $\varphi$ , but we have not actually suggested how to measure such a quantity in experiments.

To calculate  $\bar{\mathbf{M}}$ , we first write  $\Delta \mathbf{R}$  in (177) as

$$\Delta \mathbf{R} = (\hat{\mathbf{k}}\hat{\mathbf{E}}_0 - \hat{\mathbf{E}}_0\hat{\mathbf{k}})\Delta R. \quad (186)$$

To leading order we have from the first term in (171)

$$\Delta R = \frac{\alpha}{b_0} \epsilon(\sigma) \frac{\chi^3}{2\pi} \left\{ 12 \left( \ln \left[ \frac{\chi}{\sqrt{3}} \right] - \gamma_E \right) + 37 \right\}. \quad (187)$$

Since

$$\frac{\alpha}{b_0} \epsilon \chi^3 = \frac{3}{2} \chi_0 \rho \epsilon(\sigma) F^3(\sigma), \quad (188)$$

we have to leading order in (177)

$$-\Delta \mathbf{R} \cdot \bar{\mathbf{W}} \approx -\frac{\Delta \mathbf{R}}{(1 + \rho J(\sigma))^m}. \quad (189)$$

We can now calculate  $\bar{\mathbf{W}}$  to leading order in  $\chi \ll 1$  in the same way as in Sec. II. Equation (189) gives off-diagonal elements that are on the same order of magnitude as the other  $\mathcal{O}(\chi)$  terms (we do not consider large  $\ln \chi$ , because then  $\chi$  would have to be extremely small). However, we can

still neglect these off-diagonal terms if we only consider the degree of polarization, because of the following. Consider for simplicity  $m = 0$ , then [again with  $\rho = \mathcal{O}(\chi_0^0)$ ]

$$\bar{\mathbf{W}}_{(\perp)} = \mathbf{1} + \chi_0 \bar{\mathbf{W}}_{(\perp)}^{(1)} + \mathcal{O}(\chi_0^2) \quad (190)$$

and

$$\langle p_f^2 \rangle = \frac{1}{2} \|\bar{\mathbf{M}}_{(\perp)}\|_F^2 = 1 + \chi_0 \text{tr} \bar{\mathbf{W}}_{(\perp)}^{(1)} + \mathcal{O}(\chi_0^2), \quad (191)$$

so only the diagonal components contribute to leading order. We find

$$\begin{aligned} \bar{\mathbf{W}}_{(\perp)}^{(1)} &= -\frac{5}{2\sqrt{3}} [\hat{\mathbf{E}}_0 \hat{\mathbf{E}}_0 + \hat{\mathbf{k}} \hat{\mathbf{k}}] \int_{-\infty}^{\infty} d\sigma \frac{\rho F^3(\sigma)}{[1 + \rho I(\sigma)]^2} \\ &\quad + \dots \hat{\mathbf{E}}_0 \hat{\mathbf{k}} + \dots \hat{\mathbf{k}} \hat{\mathbf{E}}_0, \end{aligned} \quad (192)$$

and taking the trace gives

$$\langle p_f^2 \rangle = 1 - \frac{5\chi_0}{\sqrt{3}} \int_{-\infty}^{\infty} d\sigma \frac{\rho F^3(\sigma)}{[1 + \rho I(\sigma)]^2}. \quad (193)$$

Comparing this with (17), we see that the degree of depolarization is the same order of magnitude along  $\hat{\mathbf{B}}_0$  and in the  $\hat{\mathbf{E}}_0\text{-}\hat{\mathbf{k}}$  plane.

Next we present the  $\mathcal{O}(\chi)$  results for general  $m$ , assuming for simplicity a nonoscillating field. We will only consider the components in the  $\hat{\mathbf{E}} - \hat{\mathbf{k}}$  plane, so we omit  $\perp$  for simplicity. We order to components so that  $\hat{\mathbf{E}} \rightarrow (1, 0)$  and  $\hat{\mathbf{k}} \rightarrow (0, 1)$  within this 2D space. We use notation similar to Sec. II C,

$$\bar{\mathbf{W}}(\sigma, \chi_0, m) = \sum_{k=0}^{\infty} \bar{\mathbf{w}}_{m,k}(\sigma, \rho, \ln \chi_0) \chi_0^k, \quad (194)$$

where

$$\bar{\mathbf{w}}_{m,k} = \frac{1}{\rho^{m+k}} \bar{\omega}_{m,k}, \quad \bar{\omega}_{m,0} = \frac{1}{y^m}. \quad (195)$$

We find (omitting the subscript  $m$ ,  $\bar{\omega}_{m,k} \rightarrow \bar{\omega}_k$ , which is the same on all factors of  $\bar{\omega}$ )

$$\begin{aligned} \bar{\omega}_1 &= \int_{\sigma}^{\infty} d\sigma' F^3(\sigma') \left\{ \frac{55}{32\sqrt{3}} \partial_y^2 \bar{\omega}_0 - \frac{55}{8\sqrt{3}} \frac{\partial_y \bar{\omega}_0}{y - J(\sigma')} - \frac{5}{2\sqrt{3}} \frac{\bar{\omega}_0}{[y - J(\sigma')]^2} \right. \\ &\quad \left. + \frac{9}{\pi} \left( L + \ln \left[ \frac{F(\sigma')}{\sqrt{3}[y - J(\varphi)]} \right] - \gamma_E + \frac{37}{12} \right) \begin{pmatrix} 0 & -1 \\ 1 & 0 \end{pmatrix} \cdot \frac{\bar{\omega}_0}{[y - J(\sigma')]^2} \right\}. \end{aligned} \quad (196)$$

### B. Transseries

From the above we see that, for a linearly polarized field and an electron which has spin components in the  $\hat{\mathbf{E}} - \hat{\mathbf{k}}$  plane, the  $\chi_0 \ll 1$  expansion is not just a power series, it is a transseries with powers  $\chi_0^k$ , powers of logarithms  $[\ln \chi_0]^k$ , and terms proportional to either  $\cos(\dots/\chi_0)$  or  $\sin(\dots/\chi_0)$ . For a linearly polarized field, these spin components completely decouple from the  $\mathbf{e}_0 - \hat{\mathbf{B}}$  components, so if one averages and sums over the initial and final spins, then the  $\hat{\mathbf{E}} - \hat{\mathbf{k}}$  components do not contribute and one is left with a  $\chi_0 \ll 1$  expansion which only has powers  $\chi_0^k$ . However, for a field which is not linearly polarized, the local direction of the magnetic field at one light-front time is no longer orthogonal to the local direction of the electric field at some other light-front time,  $\hat{\mathbf{B}}(\sigma_1) \cdot \hat{\mathbf{E}}(\sigma_2) \neq 0$ , so one can in general expect coupling between the  $\hat{\mathbf{E}} - \hat{\mathbf{k}}$  and  $\mathbf{e}_0 - \hat{\mathbf{B}}$  components, which means the  $[\ln \chi_0]^k$ ,  $\cos(\dots/\chi_0)$  and  $\sin(\dots/\chi_0)$  terms in the  $\hat{\mathbf{E}} - \hat{\mathbf{k}}$  space will induce such terms also in the  $\mathbf{e}_0 - \hat{\mathbf{B}}$  space.

Consider for example a train of three Sauter pulses

$$\mathbf{a}(\sigma) = a_0[\mathbf{e}_x \tanh(\sigma + \Delta\sigma) + \mathbf{e}_y \tanh(\sigma) + \mathbf{e}_x \tanh(\sigma - \Delta\sigma)], \quad (197)$$

where  $\Delta\sigma$  is large enough so that the three pulses are well separated. If we sum over the initial and final spins, then we should project  $\mathbf{N}_0 \cdot \mathbf{W} \cdot \mathbf{N}_f$  with  $\mathbf{N}_0 = \mathbf{N}_f = \mathbf{e}_0$ . When we integrate backwards from  $\sigma = +\infty$  to  $\sigma = \Delta\sigma/2$ , only the last term in (197) contributes. In this interval the field is approximately linearly polarized with  $\hat{\mathbf{B}}(\sigma) \propto \mathbf{e}_y$ , so from (33) we see that

$$\mathbf{W}(\Delta\sigma/2) \cdot \mathbf{e}_0 = c_0 \mathbf{e}_0 + c_y \mathbf{e}_y, \quad (198)$$

where  $c_0$  and  $c_y$  are two nonzero scalars. Then we use (198) as the ‘‘initial’’ condition for integrating through the middle pulse, from  $\sigma = +\Delta\sigma/2$  to  $\sigma = -\Delta\sigma/2$ , where  $\hat{\mathbf{B}}(\sigma) \propto \mathbf{e}_x$ . The  $\mathbf{e}_0$  term in (198) will generate a  $\mathbf{e}_0$  and a  $\mathbf{e}_x$  term, and the  $\mathbf{e}_y$  term will oscillate as in (176) in the  $\mathbf{e}_y - \mathbf{e}_z$  plane. Hence, all components of

$$\mathbf{W}(-\Delta\sigma/2) \cdot \mathbf{e}_0 = d_0 \mathbf{e}_0 + d_x \mathbf{e}_x + d_y \mathbf{e}_y + d_z \mathbf{e}_z \quad (199)$$

are in general nonzero. However, when we use (199) as the initial condition for integrating through the first pulse, from  $\sigma = -\Delta\sigma/2$  to  $\sigma = -\infty$ , the  $\mathbf{e}_x$  and  $\mathbf{e}_z$  components decouple from the other two and will therefore not contribute to  $\mathbf{e}_0 \cdot \mathbf{W}(-\infty) \cdot \mathbf{e}_0$ . The  $\mathbf{e}_0$  component in (199) does contribute to  $\mathbf{e}_0 \cdot \mathbf{W}(-\infty) \cdot \mathbf{e}_0$  but does not contain any term with  $\cos \varphi$  or  $\sin \varphi$ . We are therefore interested in

$$\mathbf{e}_y \cdot \mathbf{W}(-\Delta\sigma/2) \cdot \mathbf{e}_0 \approx \cos \varphi \mathbf{e}_y \cdot \mathbf{W}(\Delta\sigma/2) \cdot \mathbf{e}_0, \quad (200)$$

which will give  $\mathbf{e}_0 \cdot \mathbf{W}(-\infty) \cdot \mathbf{e}_0$  a term proportional to  $\cos \varphi$ . To leading order in  $\chi_0 \ll 1$ , we can obtain  $\mathbf{e}_y \cdot \mathbf{W}(\Delta\sigma/2) \cdot \mathbf{e}_0$  directly from (33). Then we use (33) a second time, but replace  $\omega_{m,0} = 1/y^m$  with

$$\mathbf{e}_y \cdot \omega_{m,0} \cdot \mathbf{e}_y \rightarrow \mathbf{e}_y \cdot \mathbf{W}(-\Delta\sigma/2) \cdot \mathbf{e}_0, \quad (201)$$

while  $\mathbf{e}_0 \cdot \omega_{m,0} \cdot \mathbf{e}_y = 0$  still. In other words, we use (33) first for the third pulse and then for the first pulse, but for the first pulse  $\omega_{m,0}$  is more nontrivial due to the more nontrivial initial conditions at  $\sigma = -\Delta\sigma/2$  compared to those at  $\sigma = +\infty$ . We have thus found that  $\mathbf{e}_0 \cdot \mathbf{W}(-\infty) \cdot \mathbf{e}_0$  contains a term proportional to  $\chi_0^2 \cos \varphi$  where  $\varphi \propto 1/\chi_0$ . Although this is suppressed by a factor of  $\chi_0^2$  compared to the zeroth order, i.e. the solution to LL, it has fast oscillations which are absent at  $\mathcal{O}(\chi_0^0)$  and  $\mathcal{O}(\chi_0)$ .

## VII. CONCLUSIONS

We have derived analytical approximations for the low-energy expansion of  $\alpha$ -resummed Mueller matrices, where the LO is given by the solution to the Landau-Lifshitz equation. We have checked that these analytical approximations agree with the full numerical solution of the integro-differential equations for the moments. We have considered the locally constant, locally monochromatic, as well as more general regimes. We have showed how to factor out the fast spin precession to obtain an equation with only slowly varying terms.

We have also shown how to obtain the spectrum from the moments. This is useful since in our approach it is easier and faster to obtain the moments. We have treated  $m$  as a continuous, complex variable, which allowed us to obtain a  $\chi \ll 1$  expansion of the spectrum by performing an inverse Mellin transform. It would be interesting to go beyond this  $\chi \ll 1$  expansion and perform the Mellin integral numerically and see how much time that would take compared to solving (B1) directly. We have also shown how to use the principle of maximum entropy to obtain a good approximation of the spectrum with just a handful of integer moments and without using a  $\chi \ll 1$  expansion. Although considering integer moments already works well, it would be interesting to see if one could find an even faster convergence by considering noninteger moments or some more general expectation values,  $\langle f(kP) \rangle$ . This, and finding suitable prior distributions, will probably be useful when applying the principle of maximum entropy to cases where the spectrum looks quite different from a Gaussian, e.g. at early times where there is a very sharp peak near  $x = 0$  or for large  $\chi$ .

## ACKNOWLEDGMENTS

G. T. is supported by the Swedish Research Council, Contract No. 2020-04327. Thanks to Tom Blackburn for correspondence about [31].

### APPENDIX A: BUILDING BLOCKS

The Mueller matrices  $\mathbf{M}_L$  and  $\mathbf{M}_C$  are given by Eqs. (20)–(32) in [29], which we repeat here for the readers' convenience.

The field is a nontrivial function of light-front time, and we are working on the probability level. For each  $\mathcal{O}(\alpha)$  step (either photon emission or a loop) we therefore have two light-front-time variables,  $\phi_1^{(j)}$  and  $\phi_2^{(j)}$ , where  $j = 1, 2, \dots, n$  runs over all the steps for each  $\mathcal{O}(\alpha^n)$  contribution. We change variables to  $\sigma_j = (\phi_2^{(j)} + \phi_1^{(j)})/2$  and  $\theta_j = \phi_2^{(j)} - \phi_1^{(j)}$ . Different steps are light-front-time ordered according to  $\theta(\sigma_{j+1} - \sigma_j)$  [60]. The  $\theta_j$  integrals can be performed for each step separately. We have

$$\mathbf{M}_{C,L}(b_0, q, \sigma) = \frac{i\alpha}{2\pi b_0} \int \frac{d\theta}{\theta} \exp\left\{\frac{ir}{2b_0}\theta M^2\right\} \mathbf{R}_{C,L}, \quad (\text{A1})$$

with an integration contour above  $\theta = 0$ . The dependence on the longitudinal momentum is expressed in terms of

$$s = 1 - q, \quad r = \frac{1}{s} - 1, \quad \kappa = \frac{1}{s} + s. \quad (\text{A2})$$

The field dependence of the exponent is given by the effective mass [53]

$$M^2 = 1 + \langle \mathbf{a}^2 \rangle_\phi - \langle \mathbf{a} \rangle_\phi^2, \quad (\text{A3})$$

where

$$\langle F \rangle_\phi = \frac{1}{\theta} \int_{\phi_1}^{\phi_2} d\phi F(\phi). \quad (\text{A4})$$

The preexponential factors  $\mathbf{R}_{C,L}$  are  $4 \times 4$  matrices for photon emission and the loop. Their field dependence is expressed in terms of

$$\mathbf{w}_1 = \mathbf{a}(\phi_1) - \langle \mathbf{a} \rangle_{21}, \quad \mathbf{w}_2 = \mathbf{a}(\phi_2) - \langle \mathbf{a} \rangle_{21}, \quad (\text{A5})$$

where  $\mathbf{a} = \{a_1, a_2, 0\}$ ,  $D_1 = \mathbf{w}_1 \cdot \mathbf{w}_2$ ,

$$\mathbf{X} = \frac{1}{2}(\mathbf{w}_2 + \mathbf{w}_1), \quad \mathbf{V} = \frac{1}{2}\boldsymbol{\sigma}_2 \cdot (\mathbf{w}_2 - \mathbf{w}_1), \quad (\text{A6})$$

where

$$\boldsymbol{\sigma}_2 = \begin{pmatrix} 0 & -i & 0 \\ i & 0 & 0 \\ 0 & 0 & 0 \end{pmatrix} \quad (\text{A7})$$

and  $\mathbf{Y} = \mathbf{w}_2 - \mathbf{w}_1$ . We also define  $\mathbf{1}_\perp = \mathbf{1} - \hat{\mathbf{k}}\hat{\mathbf{k}}$ ,  $\hat{\mathbf{k}} = \{0, 0, 1\}$ . We have

$$\mathbf{R}_C = \begin{pmatrix} \langle \mathbb{R}^C \rangle & \mathbf{R}_1^C \\ \mathbf{R}_0^C & \mathbf{R}_{01}^C \end{pmatrix} \quad (\text{A8})$$

and

$$\mathbf{R}_L = \begin{pmatrix} \langle \mathbb{R}^L \rangle & \mathbf{R}_1^L \\ \mathbf{R}_0^L & \mathbf{R}_{01}^L \end{pmatrix} = \begin{pmatrix} -\langle \mathbb{R}^C \rangle & -\mathbf{R}_0^C \\ -\mathbf{R}_0^C & -\langle \mathbb{R}^C \rangle \mathbf{1} + \mathbf{R}_{01}^{\text{rot}} \end{pmatrix}, \quad (\text{A9})$$

where

$$\langle \mathbb{R}^C \rangle = \frac{\kappa}{2} \left[ \frac{2ib_0}{r\theta} + 1 + D_1 \right] - 1, \quad (\text{A10})$$

$$\mathbf{R}_0^C = q \left\{ \mathbf{1} + \left[ 1 + \frac{1}{s} \right] \hat{\mathbf{k}}\mathbf{X} \right\} \cdot \mathbf{V}, \quad (\text{A11})$$

$$\mathbf{R}_1^C = \frac{q}{s} \{ \mathbf{1} + [1 + s] \hat{\mathbf{k}}\mathbf{X} \} \cdot \mathbf{V}, \quad (\text{A12})$$

$$\mathbf{R}_{01}^C = \frac{q}{s} \left\{ \hat{\mathbf{k}}\mathbf{X} - s\mathbf{X}\hat{\mathbf{k}} - \frac{q}{2}\hat{\mathbf{k}}\hat{\mathbf{k}} \right\} + \left[ \frac{2ib_0}{r\theta} + D_1 \right] \left[ \mathbf{1}_\perp + \frac{\kappa}{2}\hat{\mathbf{k}}\hat{\mathbf{k}} \right], \quad (\text{A13})$$

and

$$\mathbf{R}_{01}^{\text{rot}} = \text{sign}(\theta) \left[ \frac{q}{2}(\mathbf{Y}\hat{\mathbf{k}} - \hat{\mathbf{k}}\mathbf{Y}) - q \left[ 1 + \frac{1}{s} \right] (\mathbf{X} \cdot \mathbf{V}) \boldsymbol{\sigma}_2 \right]. \quad (\text{A14})$$

In the LCF regime one can express the  $\theta$  integrals in terms of Airy functions,

$$\mathbf{M}_C = \frac{\alpha}{b_0} \left\{ - \left( \text{Ai}_1(\xi) + \kappa \frac{\text{Ai}'(\xi)}{\xi} \right) \mathbf{e}_0 \mathbf{e}_0 + \frac{q}{s} \frac{\text{Ai}(\xi)}{\sqrt{\xi}} \mathbf{e}_0 \hat{\mathbf{B}} + q \frac{\text{Ai}(\xi)}{\sqrt{\xi}} \hat{\mathbf{B}} \mathbf{e}_0 - \text{Ai}_1(\xi) (\mathbf{1}_\perp + [\kappa - 1] \mathbf{1}_\parallel) - \frac{\text{Ai}'(\xi)}{\xi} (2\mathbf{1}_\perp + \kappa \mathbf{1}_\parallel) \right\} \quad (\text{A15})$$

and

$$\mathbf{M}_L = \frac{\alpha}{b_0} \left\{ \left( \text{Ai}_1(\xi) + \kappa \frac{\text{Ai}'(\xi)}{\xi} \right) \mathbf{1}_4 - q \frac{\text{Ai}(\xi)}{\sqrt{\xi}} (\mathbf{e}_0 \hat{\mathbf{B}} + \hat{\mathbf{B}} \mathbf{e}_0) + q \frac{\text{Gi}(\xi)}{\sqrt{\xi}} (\hat{\mathbf{k}} \hat{\mathbf{E}} - \hat{\mathbf{E}} \hat{\mathbf{k}}) \right\}, \quad (\text{A16})$$

where

$$\text{Ai}_1(\xi) = \int_{\xi}^{\infty} dt \text{Ai}(t), \quad (\text{A17})$$

Gi is the Scorer function,

$$\frac{\text{Ai}(\xi) + i\text{Gi}(\xi)}{\sqrt{\xi}} = \int_0^{\infty} \frac{d\tau}{\pi} \exp\left\{i\xi^{3/2}\left(\tau + \frac{\tau^3}{3}\right)\right\}, \quad (\text{A18})$$

$\xi = (r/\chi(\sigma))^{2/3}$ , and  $\chi(\sigma) = |\mathbf{a}'(\sigma)|b_0$ . In 3D, the electric and magnetic field unit vectors are

$$\hat{\mathbf{E}}(\sigma) = \frac{\mathbf{a}'(\sigma)}{|\mathbf{a}'(\sigma)|}, \quad \hat{\mathbf{B}}(\sigma) = \hat{\mathbf{E}}(\sigma) \times \hat{\mathbf{k}}, \quad (\text{A19})$$

where  $\hat{\mathbf{k}} = \{0, 0, 1\}$ . The 4D version of these three vectors are simply obtained by replacing  $(v_1, v_2, v_3) \rightarrow (0, v_1, v_2, v_3)$ , e.g.

$$\hat{\mathbf{E}}(\sigma) = E_1(\sigma)\mathbf{e}_1 + E_2(\sigma)\mathbf{e}_2, \quad (\text{A20})$$

where

$$\begin{aligned} \mathbf{e}_0 &= \{1, 0, 0, 0\}, & \mathbf{e}_1 &= \{0, 1, 0, 0\}, \\ \mathbf{e}_2 &= \{0, 0, 1, 0\}, & \mathbf{e}_3 &= \{0, 0, 0, 1\}. \end{aligned} \quad (\text{A21})$$

We also have  $\mathbf{1}_4 = \sum_{j=1}^4 \mathbf{e}_j \mathbf{e}_j$  and

$$\mathbf{1}_{\perp} = \hat{\mathbf{E}}\hat{\mathbf{E}} + \hat{\mathbf{B}}\hat{\mathbf{B}} = \mathbf{e}_1\mathbf{e}_1 + \mathbf{e}_2\mathbf{e}_2, \quad \mathbf{1}_{\parallel} = \mathbf{e}_3\mathbf{e}_3. \quad (\text{A22})$$

In the LMF regime one can express the  $\theta$  integrals in terms of Bessel functions (see [25]).

## APPENDIX B: LCF OF SPECTRUM

$x$  is related to the final momentum as in (4). The cumulative function  $\mathbf{M}(b_0, x)$  can be obtained from [29]

$$\begin{aligned} \frac{\partial \mathbf{M}}{\partial \sigma} &= - \int_0^1 dq \left\{ \mathbf{M}^L \cdot \mathbf{M}(b_0, x) \right. \\ &\quad \left. + \theta(x-q)\mathbf{M}^C \cdot \mathbf{M}\left([1-q]b_0, \frac{x-q}{1-q}\right) \right\}, \end{aligned} \quad (\text{B1})$$

with

$$\mathbf{M}(\sigma \rightarrow +\infty) = \mathbf{M}^{(0)} = \mathbf{1}. \quad (\text{B2})$$

To obtain a  $\chi \ll 1$  approximation of the spectrum, we start by differentiating (B1) with respect to  $x$ , to obtain an equation directly in terms of the spectrum  $\mathbf{S} = \partial_x \mathbf{M}$ ,

$$\begin{aligned} \frac{\partial \mathbf{S}}{\partial \sigma} &= - \int_0^1 dq \left\{ \mathbf{M}_L \cdot \mathbf{S}(b_0, x) \right. \\ &\quad \left. + \frac{\theta(x-q)}{1-q} \mathbf{M}_C \cdot \mathbf{S}\left[(1-q)b_0, \frac{x-q}{1-q}\right] \right\} \\ &\quad - \mathbf{M}_C(b_0, q=x) \cdot \mathbf{M}[(1-x)b_0, 0]. \end{aligned} \quad (\text{B3})$$

This is the generalization of Eq. (94) in [29], which is the corresponding equation for a constant field, to nonconstant fields. After some initial period of time,  $\mathbf{M}[(1-x)b_0, 0]$  becomes exponentially suppressed, and we can hence neglect it in (B3). To find an approximation we make a similar ansatz as in [29],

$$\mathbf{S} = \frac{e^{-X^2}}{\sqrt{\pi\chi_0\lambda}} \sum_{n=0}^{\infty} \rho_n \chi_0^{n/2}, \quad (\text{B4})$$

where, instead of the spectrum variable  $x$ , we use

$$X = \frac{x - x_{cl}}{\sqrt{\chi_0\lambda}}. \quad (\text{B5})$$

$X$ ,  $\lambda$ , and  $\rho$  depend only on  $\chi_0$  via  $\rho$ , but in this expansion we consider  $\rho = \mathcal{O}(1)$ . We can think of  $\rho$  as independent of the expansion parameter  $\chi_0$ , but we have to remember to still make the shift  $\rho \rightarrow (1-q)\rho$  in the second term in (B3). We could determine everything about this expansion of  $\mathbf{S}$  without relying on any previous knowledge about  $\mathbf{S}$ , but we do in fact already know some things about  $\mathbf{S}$  which allow us to skip some steps. For example, we could determine  $x_{cl}$ , but we already know that it has to be consistent with the solution to LL, which means

$$x_{cl} = 1 - \frac{kP_{LL}}{b_0} = \frac{\rho J(\sigma)}{1 + \rho J(\sigma)}. \quad (\text{B6})$$

We have also used the fact that this expansion has to reduce to the constant-field result in [29] to write  $\mathcal{E}(X^2) = e^{-X^2}/\sqrt{\pi}$ . We also set  $\rho_0 = \mathbf{1}$ . The ultimate justification for (B4) is the fact that it works; i.e. if the spectrum did not have this mathematical structure, we would not be able to find functions  $\lambda$  and  $\rho$  such that it solves (B3) to each order in the expansion in  $\chi_0$ .

Expanding (B3) we find that the terms which would otherwise have been the leading order vanish since we have already used (B6). At next order in  $\mathcal{O}(\sqrt{\chi_0})$ ,  $\rho_0 = \mathbf{1}$  is still the only  $\rho_n$  that contributes at this order, which means there is only one rather than four equations, and things simplify further compared to [29] since we have already used  $\mathcal{E}(X^2) = e^{-X^2}/\sqrt{\pi}$ . After dividing the equation by  $e^{-X^2}$ , we find one term that does not depend on  $X$  and one that is quadratic in  $X$ ,  $f_0(\sigma, \rho) + f_2(\sigma, \rho)X^2 = 0$ . Both terms have to be zero independently, since  $x$  only appears in  $X$ . But at this order we only have one unknown function,  $\lambda$ .

Fortunately, we find  $f_2(\sigma, \rho)/f_0(\sigma, \rho) = -2$ , so if  $f_0(\sigma, \rho) = 0$ , then  $f_2(\sigma, \rho) = 0$  automatically. This is one consistency check that (B4) is correct. We thus have one independent equation for one unknown,

$$\partial_\sigma \lambda - \rho F^2 [\rho \partial_\rho \lambda + 3\lambda] + \frac{55}{8\sqrt{3}} (1 - x_{cl})^4 \rho F^3 = 0. \quad (\text{B7})$$

To make this an ordinary differential equation, we again change variables from  $\sigma$  and  $\rho$  to  $\sigma$  and  $y$  in (15),

$$\partial_\sigma \frac{\lambda(\sigma, y)}{[y - J(\sigma)]^3} = -\frac{55F^3(\sigma)}{8\sqrt{3}y^4}. \quad (\text{B8})$$

Thus,  $\lambda$  is given by (38). We have  $\lambda(\sigma \rightarrow -\infty) = 2S^2/\chi_0$ , where the standard deviation  $S^2$  is given by (21).

### APPENDIX C: COMPARISON WITH LITERATURE

As shown in [29], once we have obtained the result for a wave packet which is initially sharply (infinitely) peaked, we can use that result as a Green's function for obtaining the corresponding result for cases when the initial wave packet has a finite width. Therefore, to compare with the results in [31] we set the initial variance to zero. We immediately see that (21) agrees with Eq. (14) in [31], which was obtained there with a very different approach.

The  $\{1, 0\} \cdot \mathbf{w}_{1,1} \cdot \{1, 0\}$  component in (18) gives the first moment after averaging and summing over initial and final spins. We can compare this component with the equations in [31] as follows. Equation (10) in [31] gives an ordinary, rather than partial, differential equation for the first moment, denoted there as  $\mu$ , coupled to higher-order moments, the variance  $\sigma$ , etc. After expanding that equation to first order in  $\chi_0$  one finds an equation which couples  $\mu$  to only  $\sigma$  and no higher-order moments,

$$0 = -\hat{\mu}'_{(0)} - \frac{2}{3} R_c |f|^2 \hat{\mu}_{(0)}^2 + \chi_0 \left( -\hat{\mu}'_{(1)} - \frac{2}{3} R_c |f|^2 [2\hat{\mu}_{(1)} \hat{\mu}_{(0)} + \hat{\sigma}_{(1)}^2] + \frac{55R_c}{8\sqrt{3}} |f|^3 \hat{\mu}_{(0)}^3 \right), \quad (\text{C1})$$

where we have used essentially the same notation as in [31]. To translate to our notation use  $(2/3)R_c \rightarrow \rho$  and  $|f| \rightarrow F$ . The first two terms determine  $\hat{\mu}_{(0)}$  as the solution to LL, and  $\hat{\sigma}_{(1)}$  is given by Eq. (14) in [31]. One can then integrate the  $\mathcal{O}(\chi_0)$  part of (C1) to find  $\hat{\mu}_{(1)}$ . Since  $\hat{\sigma}_{(1)}$  already contains an integral over  $\phi$ , one might have guessed that the result would contain more integrals compared to (18), but it is possible to simplify using partial integration. The resulting  $\hat{\mu}_{(1)}$  agrees exactly with the  $\{1, 0\} \cdot \mathbf{w}_{1,1} \cdot \{1, 0\}$  component in (18).

### APPENDIX D: OSCILLATING TERMS IN $\bar{\mathbf{W}}$

The oscillating terms in (180),  $\mathbf{M}'_{C,O}$ , oscillate rapidly for  $\chi \ll 1$ . This fact alone does not mean that one can neglect  $\mathbf{M}'_{C,O}$ , because e.g. a  $\cos(2\varphi)$  term in  $\mathbf{W}$  might combine with  $\cos(2\varphi)$  in  $\mathbf{M}'_{C,O}$  to give something non-negligible after integrating over  $\sigma$ . However,  $\mathbf{M}'_{C,O}$  is negligible anyway as the following shows. Since  $b - a$  in (180) is small for  $\chi \ll 1$ , we can treat  $\mathbf{M}'_{C,O}$  in perturbation theory. We can still use the ansatz in (194), where we now have two combinations,  $\ln(\chi_0/\rho)$  and  $\varphi$ , which depend on the order of magnitude of  $\chi_0$  but which are unaffected by  $b_0 \rightarrow (1 - q)b_0$  since the factors of  $1 - q$  cancel in  $\chi_0/\rho$ . We find that we should add to (196)

$$\Delta \bar{\omega}_{m,1} = \frac{5\sqrt{3}}{48} \int_\sigma^\infty d\sigma' \frac{F^3(\sigma')}{[y - J(\sigma')]^2} \times \begin{pmatrix} -\cos(2\varphi[\sigma']) & \sin(2\varphi[\sigma']) \\ \sin(2\varphi[\sigma']) & \cos(2\varphi[\sigma']) \end{pmatrix} \cdot \bar{\omega}_{m,0}. \quad (\text{D1})$$

Unlike the other terms in (196), which are  $\mathcal{O}(\chi_0^0)$  [or  $\mathcal{O}(\ln \chi_0)$ ],  $\Delta \bar{\omega}_{m,1}$  is actually higher order in  $\chi_0$  due to the highly oscillatory integrand. Let  $g$  stand for the part of the integrand in (D1) outside the matrix. We can perform partial integration to extract the leading order as

$$\begin{aligned} & \int_\sigma^\infty d\sigma' \{ \cos(2\varphi[\sigma']), \sin(2\varphi[\sigma']) \} g(\sigma') \\ &= \{ -\sin 2\varphi, \cos 2\varphi \} \frac{g}{2\varphi'} \\ & \quad - \{ \cos 2\varphi, \sin 2\varphi \} \frac{1}{2\varphi'} \partial_\sigma \frac{g}{2\varphi'} \\ & \quad - \int_\sigma^\infty d\sigma' \{ \cos 2\varphi, \sin 2\varphi \} \partial_{\sigma'} \frac{1}{2\varphi'} \partial_{\sigma'} \frac{g}{2\varphi'}, \end{aligned} \quad (\text{D2})$$

where all the boundary terms are evaluated at  $\sigma$ . Note that  $1/\varphi' \propto \chi_0$ , so the first boundary term is  $\mathcal{O}(\chi_0)$  and the second one is  $\mathcal{O}(\chi_0^2)$ . Both boundary terms vanish for  $\sigma \rightarrow -\infty$ , so  $\chi_0 \Delta \bar{\omega}_{m,1}$  must be at least  $\mathcal{O}(\chi_0^3)$ . Since each partial integration brings a factor of  $1/\varphi' \propto 1/F$ , if we tried to perform further partial integrations in the same way we would end up with an integrand that has too many powers of  $1/F$  and hence does not converge. However, we can split the integral in the last line of (D2) into  $\int_\sigma^0 + \int_0^\infty$  and use  $\sin 2\varphi = (1/[2\varphi']) d_\sigma [1 - \cos 2\varphi]$  for the second part and similarly for the first part, and then perform partial integration a third time. Thus, e.g. for experimental purposes, it seems safe to neglect  $\chi_0 \Delta \bar{\omega}_{m,1}$ . For studying the transseries structure, though, it may be interesting to note that  $\Delta \bar{\omega}_{m,1}(\sigma \rightarrow -\infty)$  gives terms proportional to  $\cos(2\varphi[-\infty] + \delta)$ , which combined with the overall rotation (176) give terms which oscillate 3 times as fast  $\cos(3\varphi + \dots)$ .

There is a contribution to  $\bar{\omega}_{m,2}$  which also involves a single factor of  $\mathbf{M}'_{C,O}$ . It can be shown to be negligible in the same way as for  $\Delta\bar{\omega}_{m,1}$ . Indeed,  $\chi_0^2\bar{\omega}_{m,2}$  already comes with an extra factor of  $\chi_0$  compared to  $\chi_0\bar{\omega}_{m,1}$ , so a small contribution to  $\bar{\omega}_{m,2}$  means a very small contribution to  $\bar{\mathbf{W}}$ . In contrast to  $\bar{\omega}_{m,1}$ , there is another contribution to  $\bar{\omega}_{m,2}$  which involves two factors of  $\mathbf{M}'_{C,O}$ , which can be written as

$$\Delta\bar{\omega}_{m,2} = \frac{5\sqrt{3}}{48} \int_{\sigma}^{\infty} d\sigma' \frac{F^3(\sigma')}{[y - J(\sigma')]^2} \times \begin{pmatrix} -\cos(2\varphi[\sigma']) & \sin(2\varphi[\sigma']) \\ \sin(2\varphi[\sigma']) & \cos(2\varphi[\sigma']) \end{pmatrix} \cdot \bar{\omega}_{m,1}, \quad (\text{D3})$$

which can be obtained from (D1) by just replacing  $\bar{\omega}_{m,0} \rightarrow \bar{\omega}_{m,1}$  and  $\bar{\omega}_{m,1} \rightarrow \bar{\omega}_{m,2}$ . To leading order  $\Delta\bar{\omega}_{m,1}$  is obtained from the first boundary term in (D2), which gives

$$\begin{pmatrix} -\cos(2\varphi) & \sin(2\varphi) \\ \sin(2\varphi) & \cos(2\varphi) \end{pmatrix} \begin{pmatrix} \sin(2\varphi) & \cos(2\varphi) \\ \cos(2\varphi) & -\sin(2\varphi) \end{pmatrix} = \begin{pmatrix} 0 & -1 \\ 1 & 0 \end{pmatrix}. \quad (\text{D4})$$

It is therefore much easier to calculate  $\Delta\bar{\omega}_{m,2}$  to leading order compared to  $\Delta\bar{\omega}_{m,1}$ . We find

$$\chi_0^2\Delta\bar{\omega}_{m,2} = \frac{25\pi}{1152} \frac{\rho\chi_0^3}{[1 + \rho J]^m} \begin{pmatrix} 0 & 1 \\ -1 & 0 \end{pmatrix} \int \frac{d\sigma F^5}{[1 + \rho I]^4}. \quad (\text{D5})$$

So,  $\chi_0^2\Delta\bar{\omega}_{m,2}$  is actually not smaller than  $\chi_0\Delta\bar{\omega}_{m,1}$ . However, the important point is that  $\chi_0^2\Delta\bar{\omega}_{m,2}$  scales as  $\chi_0^3$ , which is indeed negligible compared to the leading quantum correction which scales as  $\chi_0$ .

- 
- [1] C. S. Shen and D. White, Energy straggling and radiation reaction for magnetic bremsstrahlung, *Phys. Rev. Lett.* **28**, 455 (1972).
- [2] I. V. Sokolov, N. M. Naumova, J. A. Nees, and G. A. Mourou, Pair creation in QED-strong pulsed laser fields interacting with electron beams, *Phys. Rev. Lett.* **105**, 195005 (2010).
- [3] N. V. Elkina, A. M. Fedotov, I. Y. Kostyukov, M. V. Legkov, N. B. Narozhny, E. N. Nerush, and H. Ruhl, QED cascades induced by circularly polarized laser fields, *Phys. Rev. ST Accel. Beams* **14**, 054401 (2011).
- [4] N. Neitz and A. Di Piazza, Stochasticity effects in quantum radiation reaction, *Phys. Rev. Lett.* **111**, 054802 (2013).
- [5] N. Neitz and A. Di Piazza, Electron-beam dynamics in a strong laser field including quantum radiation reaction, *Phys. Rev. A* **90**, 022102 (2014).
- [6] C. P. Ridgers, T. G. Blackburn, D. Del Sorbo, L. E. Bradley, C. Slade-Lowther, C. D. Baird, S. P. D. Mangles, P. McKenna, M. Marklund, C. D. Murphy, and A. G. R. Thomas, Signatures of quantum effects on radiation reaction in laser-electron-beam collisions, *J. Plasma Phys.* **83**, 715830502 (2017).
- [7] F. Niel, C. Riconda, F. Amiranoff, R. Ducloux, and M. Grech, From quantum to classical modeling of radiation reaction: A focus on stochasticity effects, *Phys. Rev. E* **97**, 043209 (2018).
- [8] A. I. Nikishov and V. I. Ritus, Quantum processes in the field of a plane electromagnetic wave and in a constant field I, *Sov. Phys. JETP* **19**, 529 (1964).
- [9] V. I. Ritus, Quantum effects of the interaction of elementary particles with an intense electromagnetic field, *J. Russ. Laser Res.* **6**, 497 (1985).
- [10] A. Gonoskov, T. G. Blackburn, M. Marklund, and S. S. Bulanov, Charged particle motion and radiation in strong electromagnetic fields, *Rev. Mod. Phys.* **94**, 045001 (2022).
- [11] A. Di Piazza, C. Muller, K. Z. Hatsagortsyan, and C. H. Keitel, Extremely high-intensity laser interactions with fundamental quantum systems, *Rev. Mod. Phys.* **84**, 1177 (2012).
- [12] A. Fedotov, A. Ilderton, F. Karbstein, B. King, D. Seipt, H. Taya, and G. Torgrimsson, Advances in QED with intense background fields, *Phys. Rep.* **1010**, 1 (2023).
- [13] D. Del Sorbo, D. Seipt, T. G. Blackburn, A. G. R. Thomas, C. D. Murphy, J. G. Kirk, and C. P. Ridgers, Spin polarization of electrons by ultraintense lasers, *Phys. Rev. A* **96**, 043407 (2017).
- [14] D. Del Sorbo, D. Seipt, A. G. R. Thomas, and C. P. Ridgers, Electron spin polarization in realistic trajectories around the magnetic node of two counter-propagating, circularly polarized, ultra-intense lasers, *Plasma Phys. Controlled Fusion* **60**, 064003 (2018).
- [15] D. Seipt, D. Del Sorbo, C. P. Ridgers, and A. G. R. Thomas, Ultrafast polarization of an electron beam in an intense bichromatic laser field, *Phys. Rev. A* **100**, 061402 (2019).
- [16] Y. Y. Chen, P. L. He, R. Shaisultanov, K. Z. Hatsagortsyan, and C. H. Keitel, Polarized positron beams via intense two-color laser pulses, *Phys. Rev. Lett.* **123**, 174801 (2019).
- [17] Y. F. Li, R. Shaisultanov, K. Z. Hatsagortsyan, F. Wan, C. H. Keitel, and J. X. Li, Ultrarelativistic electron beam polarization in single-shot interaction with an ultraintense laser pulse, *Phys. Rev. Lett.* **122**, 154801 (2019).
- [18] Y. F. Li, R. Shaisultanov, Y. Y. Chen, F. Wan, K. Z. Hatsagortsyan, C. H. Keitel, and J. X. Li, Polarized ultrashort brilliant multi-GeV  $\gamma$  rays via single-shot laser-electron interaction, *Phys. Rev. Lett.* **124**, 014801 (2020).
- [19] Y. F. Li, Y. Y. Chen, W. M. Wang, and H. S. Hu, Production of highly polarized positron beams via helicity transfer from polarized electrons in a strong laser field, *Phys. Rev. Lett.* **125**, 044802 (2020).

- [20] Y. Tang, Z. Gong, J. Yu, Y. Shou, and X. Yan, Radiative polarization dynamics of relativistic electrons in an intense electromagnetic field, *Phys. Rev. A* **103**, 042807 (2021).
- [21] Y. F. Li, Y. Y. Chen, K. Z. Hatsagortsyan, A. Di Piazza, M. Tamburini, and C. H. Keitel, Strong signature of one-loop self-energy in polarization resolved nonlinear Compton scattering, *Phys. Rev. D* **107**, 116020 (2023).
- [22] Q. Qian, D. Seipt, M. Vranic, T. E. Grismayer, T. G. Blackburn, C. P. Ridgers, and A. G. R. Thomas, Parametric study of the polarization dependence of nonlinear Breit–Wheeler pair creation process using two laser pulses, *Phys. Plasmas* **30**, 103107 (2023).
- [23] V. Dinu and G. Torgrimsson, Single and double nonlinear Compton scattering, *Phys. Rev. D* **99**, 096018 (2019).
- [24] V. Dinu and G. Torgrimsson, Approximating higher-order nonlinear QED processes with first-order building blocks, *Phys. Rev. D* **102**, 016018 (2020).
- [25] G. Torgrimsson, Loops and polarization in strong-field QED, *New J. Phys.* **23**, 065001 (2021).
- [26] G. Torgrimsson, Resummation of quantum radiation reaction in plane waves, *Phys. Rev. Lett.* **127**, 111602 (2021).
- [27] G. Torgrimsson, Resummation of quantum radiation reaction and induced polarization, *Phys. Rev. D* **104**, 056016 (2021).
- [28] G. Torgrimsson, Resummation of the  $\alpha$  expansion for nonlinear pair production by an electron in a strong electromagnetic field, *Phys. Rev. D* **107**, 016019 (2023).
- [29] G. Torgrimsson, Quantum radiation reaction spectrum of electrons in plane waves, *Phys. Rev. D* **109**, 076030 (2024).
- [30] D. Seipt and A. G. R. Thomas, Kinetic theory for spin-polarized relativistic plasmas, *Phys. Plasmas* **30**, 093102 (2023).
- [31] T. G. Blackburn, Analytical solutions for quantum radiation reaction in high-intensity lasers, *Phys. Rev. A* **109**, 022234 (2024).
- [32] V. Dinu, Exact final state integrals for strong field QED, *Phys. Rev. A* **87**, 052101 (2013).
- [33] T. Heinzl, B. King, and A. J. Macleod, The locally monochromatic approximation to QED in intense laser fields, *Phys. Rev. A* **102**, 063110 (2020).
- [34] D. Seipt and B. Kampfer, Non-linear Compton scattering of ultrashort and ultraintense laser pulses, *Phys. Rev. A* **83**, 022101 (2011).
- [35] T. G. Blackburn, B. King, and S. Tang, Simulations of laser-driven strong-field QED with Ptarmigan: Resolving wavelength-scale interference and  $\gamma$ -ray polarization, *Phys. Plasmas* **30**, 093903 (2023).
- [36] H. H. Song, W. M. Wang, and Y. T. Li, Generation of polarized positron beams via collisions of ultrarelativistic electron beams, *Phys. Rev. Res.* **3**, 033245 (2021).
- [37] Z. Gao and W. M. Wang, Polarized  $\gamma$ -photon beams produced by collision of two ultrarelativistic electron beams, *Phys. Rev. A* **110**, 013502 (2024).
- [38] W. H. McMaster, Matrix representation of polarization, *Rev. Mod. Phys.* **33**, 8 (1961).
- [39] A. Di Piazza, Exact solution of the Landau-Lifshitz equation in a plane wave, *Lett. Math. Phys.* **83**, 305 (2008).
- [40] H. Heintzmann and M. Grewing, Acceleration of charged particles and radiation-reaction in strong plane and spherical waves, *Z. Phys.* **251**, 77 (1972).
- [41] A. A. Sokolov and I. M. Ternov, On polarization and spin effects in the theory of synchrotron radiation, *Sov. Phys. Dokl.* **8**, 1203 (1964).
- [42] V. N. Baier, Radiative polarization of electrons in storage rings, *Sov. Phys. Usp.* **14**, 695 (1972).
- [43] O. Costin and G. V. Dunne, Resurgent extrapolation: Rebuilding a function from asymptotic data. Painlevé I, *J. Phys. A* **52**, 445205 (2019).
- [44] G. Álvarez and H. J. Silverstone, A new method to sum divergent power series: educated match, *J. Phys. Comm.* **1**, 025005 (2017).
- [45] H. Mera, T. G. Pedersen, and B. K. Nikolić, Fast summation of divergent series and resurgent transseries from Meijer-G approximants, *Phys. Rev. D* **97**, 105027 (2018).
- [46] A. M. Shalaby, Extrapolating the precision of the hypergeometric resummation to strong couplings with application to the  $\mathcal{PT}$ —symmetric  $i\phi^3$  field theory, *Int. J. Mod. Phys. A* **35**, 2050041 (2020).
- [47] G. Torgrimsson, Nonlinear photon trident versus double Compton scattering and resummation of one-step terms, *Phys. Rev. D* **102**, 116008 (2020).
- [48] E. T. Jaynes, Information theory and statistical mechanics, *Phys. Rev.* **106**, 620 (1957).
- [49] E. T. Jaynes, Prior probabilities, *IEEE Trans. Syst. Sci. Cybern.* **4**, 227 (1968).
- [50] L. R. Mead and N. Papanicolaou, Maximum entropy in the problem of moments, *J. Math. Phys. (N.Y.)* **25**, 2404 (1984).
- [51] P. L. Novi Inverardi and A. Tagliani, Maximum entropy density estimation from fractional moments, *Commun. Stat.* **32**, 327 (2003).
- [52] X. Zhang, Y. M. Lwa, and C. G. Koh, Maximum entropy distribution with fractional moments for reliability analysis, *Struct. Saf.* **83**, 101904 (2020).
- [53] T. W. B. Kibble, A. Salam, and J. A. Strathdee, Intensity dependent mass shift and symmetry breaking, *Nucl. Phys.* **B96**, 255 (1975).
- [54] R. Gonzo and A. Ilderton, Wave scattering event shapes at high energies, *J. High Energy Phys.* **10** (2023) 108.
- [55] A. Ilderton, B. King, and S. Tang, Loop spin effects in intense background fields, *Phys. Rev. D* **102**, 076013 (2020).
- [56] V. N. Baier and V. M. Katkov, Processes involved in the motion of high energy particles in a magnetic field, *J. Exp. Theor. Phys.* **26**, 854 (1968).
- [57] V. I. Ritus, Radiative effects and their enhancement in an intense electromagnetic field, *J. Exp. Theor. Phys.* **30**, 1181 (1970).
- [58] L. H. Thomas, The motion of the spinning electron, *Nature (London)* **117**, 514 (1926).
- [59] V. Bargmann, L. Michel, and V. L. Telegdi, Precession of the polarization of particles moving in a homogeneous electromagnetic field, *Phys. Rev. Lett.* **2**, 435 (1959).
- [60] V. Dinu and G. Torgrimsson, Trident pair production in plane waves: Coherence, exchange, and spacetime inhomogeneity, *Phys. Rev. D* **97**, 036021 (2018).